RSC Advances

PAPER

View Article Online
View Journal | View Issue

Cite this: *RSC Adv.*, 2025, **15**, 11975

Immobilization of lead and zinc in contaminated soil using taro stem-derived biochar and apatite amendments: a comparative study of application ratios and pyrolysis temperatures†

Truong Xuan Vuong, * Duc Phuong Nguyen, Vu Huyen Ngoc Nguyen, Thi Thu Ha Pham and Thi Thu Thuy Nguyen

Soil contamination by heavy metals presents a substantial environmental challenge. Remediation strategies employing biochar and apatite offer promise for restoring compromised sites. However, the efficacy of apatite and biochar derived from various biomass sources remains an under-investigated area. Taro stem-derived biochar produced at 300 and 500 °C (TSB300 and TSB500) and apatite amendments were incubated in contaminated soil for one month at various ratios (biochar 3%, 6%, 10%, mixture of biochar/apatite 3 : 3%, and 6 : 6% w/w) to investigate their potential to immobilize Pb and Zn. The initial concentrations of Pb and Zn in the contaminated soil were 4165.1 ± 19.6 mg kg^{-1} and 3424.9 ± 20.4 mg kg^{-1}, respectively. Soil samples were subjected to Tessier's sequential extraction for analysis of Pb and Zn in five chemical fractions (F1: exchangeable fraction; F2: carbonate fraction; F3: Fe/Mn oxide fraction; F4: organic carbon fraction and F5: residual fraction). The results indicated that one-month biochar and/or apatite amendment significantly increased soil pH, organic carbon (OC), and electrical conductivity (EC) compared to the control ($p < 0.05$). Amendments also notably reduced exchangeable fractions of Pb and Zn (F1) up to 71.8% and 61.5%, respectively, while enhancing their presence in more stable fractions (F4 and F5). This immobilization effect peaked at the 10% biochar application and 6 : 6% biochar–apatite combination. These findings suggest that TSB300, TSB500, and their blends with apatite hold promise for immobilizing Pb and Zn in heavily contaminated soil, potentially mitigating environmental risks.

Received 7th February 2025
Accepted 7th April 2025

DOI: 10.1039/d5ra00912j

rsc.li/rsc-advances

1. Introduction

The global spread of heavy metal (HM) pollution has escalated significantly due to rapid industrial growth, urbanization, and certain human activities, such as mining, agricultural practices, and industrial waste disposal.[1,2] These activities have led to a substantial increase in soil contamination, posing serious threats to ecosystems, public health, and food security.[3–6] Heavy metals (HMs) are non-biodegradable and can persist in the soil, entering the food chain *via* contaminated soil, water, and air. Once inside organisms, these metals accumulate through bio-accumulation, endangering human and animal health.[7,8] Therefore, effective remediation strategies are necessary to reduce the concentration of HMs and improve soil quality. The impact of HMs on soil is influenced by factors such as metal concentration, chemical composition, and the surrounding environmental conditions. Merely measuring the total metal content in soil does not provide a full understanding of their availability or potential risks. Instead, chemical speciation, examining how metals interact with different components in the soil, offers a clearer picture of their behavior, movement, and toxicity.[9,10] Sequential extraction methods, such as Tessier's Sequential Extraction Procedure (TSEP), are valuable tools in this context. TSEP provides insight into the bioavailability, toxicity, and redistribution of metals by fractionating them into distinct chemical binding states: exchangeable (F1), carbonate (F2), iron/manganese oxide (F3), organic matter (F4), and residual (F5) fractions.[11,12] This approach has become integral to environmental research, offering a comprehensive understanding of metal speciation in contaminated soils.[9,10]

To address heavy metal contamination, various remediation techniques have been explored, including physical, chemical, and biological approaches. Among these, the immobilization of HMs using amendments, both organic and inorganic, has emerged as a cost-effective, rapid, and environmentally friendly strategy.[13] This approach stabilizes metals, limiting their mobility and bioavailability in the soil. One promising

Faculty of Chemistry, TNU-University of Science, Tan Thinh Ward, Thai Nguyen City 24000, Vietnam. E-mail: xuanvt@tnusedu.vn

† Electronic supplementary information (ESI) available. See DOI: https://doi.org/10.1039/d5ra00912j

amendment is biochar, a carbon-rich material produced through the pyrolysis of organic biomass in low-oxygen conditions,[14] Biochar has gained considerable attention as an effective tool for heavy metal remediation due to its large surface area, high porosity, and negative charge, which enable it to adsorb and immobilize metal ions.[15,16] Additionally, biochar's neutral to alkaline pH promotes the precipitation of metals, further limiting their mobility and bioavailability. Research has consistently demonstrated the effectiveness of biochar in mitigating heavy metal contamination in various soil types.[16–18]

In addition, recent studies have focused on enhancing biochar's effectiveness by combining it with other materials, such as apatite. Apatite, a phosphate-rich mineral, can immobilize heavy metals by forming insoluble metal-phosphate complexes, further reducing the mobility of contaminants in soil.[19,20] Apatite minerals, especially calcium phosphate, are effective in immobilizing lead (Pb) in contaminated soils by forming stable lead-phosphate complexes, which significantly reduce lead's bioavailability and mobility, making them valuable for lead remediation.[21] However, apatite's effectiveness is less pronounced for other heavy metals, such as zinc (Zn), suggesting selective interactions that limit its applicability in diverse environments.[22] Modifying apatite to fluorapatite enhances its metal retention capacity by providing additional binding sites, improving its ability to stabilize lead more effectively than hydroxyapatite.[23] Apatite also offers environmental sustainability benefits, as its application does not produce harmful byproducts and has minimal impact on soil microbial communities.[21] However, in acidic soils, apatite can dissolve, releasing immobilized lead back into the soil solution, and competing ions such as calcium, iron, and aluminium may hinder its heavy metal retention.[24] The combination of biochar with apatite has been explored to overcome these limitations.[11,18] Biochar enhances heavy metal adsorption through its high surface area and functional groups, providing more binding sites and improving metal retention.[25] It also acts as a pH buffer, preventing apatite dissolution in acidic conditions and mitigating the effects of competing ions.[18] This synergy enhances heavy metal immobilization and improves the long-term stability of remediation efforts.[26]

Heavy metal contamination, particularly lead (Pb) and zinc (Zn), is a significant environmental concern in areas surrounding Pb/Zn mining sites, such as Hich village, Dong Hy district, Vietnam.[27] These anthropogenic activities pose a substantial risk to human health and environmental stability. While various remediation strategies have been explored, the use of biochar derived from agricultural waste combined with apatite offers a promising yet underexplored approach in these regions.[11,28] Despite the potential of this method, there is a lack of detailed studies examining the effects of combining apatite with biochar from different sources for heavy metal immobilization. Previous studies have explored the combination of apatite with biochar derived from materials such as rice straw,[11] corncob,[29] peanut shells,[30] pomelo peel,[10] and sugarcane bagasse.[10] However, the combination of apatite with biochar derived from taro stems (*Colocasia esculenta*) remains unexplored. Taro stems, abundant and fast-growing in tropical regions like Vietnam, were selected as a feedstock for biochar production due to their high organic matter content and moisture, which make them particularly suitable for pyrolysis. Unlike traditional biochar feedstocks, such as wood and rice straw, which are primarily composed of cellulose, taro stems offer a different biomass profile. This study aims to fill this gap by investigating the potential of apatite–biochar combinations from taro stems for heavy metal immobilization.

The primary objective of this investigation is to evaluate the effectiveness of biochar produced from taro stem biomass, along with a biochar–apatite blend, in affecting the chemical speciation of heavy metals in contaminated soil. Taro, a plant abundant in tropical regions such as Vietnam, provides a sustainable source for biochar production. This study hypothesizes that biochar derived from taro stems, in combination with apatite, can immobilize heavy metals and transform them into more stable chemical forms, reducing their mobility and bioavailability in contaminated soil.

The specific objectives of this study are as follows: (i) investigate the physical and chemical properties of taro stem-derived biochar pyrolyzed at 300 °C and 500 °C; (ii) examine the influence of biochar on soil properties, including pH, organic carbon content, and electrical conductivity, and explore their interactions with the exchangeable fraction of heavy metals. (iii) Assess the effects of biochar type, apatite application, and application rates on the speciation of heavy metals in contaminated soil.

2. Materials and methods

2.1. Sample gathering and experiment setup

Surface soil samples (approximately 2 kg each) were obtained from a ricefield situated near a Pb/Zn mine in Thai Nguyen Province, northern Vietnam (21°43′46.27″N, 105°51′2.75″E). The samples encompass a depth of 0–20 cm and have lateral dimensions of 30 cm × 30 cm. The soil sampled from a cornfield in Hich village, Dong Hy district, Vietnam, exhibits elevated levels of lead (Pb) and zinc (Zn) due to historical mining activities, making these metals the primary contaminants of concern. While other metals, such as copper (Cu), cadmium (Cd), chromium (Cr), and arsenic (As), are also present, their concentrations are significantly lower than those of Pb and Zn.[27] This study focuses on Pb and Zn due to their higher concentrations and the greater environmental and health risks they pose. The taro used in this study was purchased from a local supermarket in Dong Hy district, Vietnam. The taro stalk was first washed with deionized water to remove contaminants. The stem of the taro stalk (*Colocasia esculenta*) was subsequently air-dried for 72 hours to achieve a consistent moisture content. Pyrolysis was carried out in a furnace oven under anaerobic conditions at 300 °C and 500 °C for 1 hour at each temperature. The furnace used was an LHTCT 08/16/C550 (Nabertherm, Germany), connected to a nitrogen gas supply to ensure anaerobic conditions during biochar production. The biochar samples derived from taro stalks at 300 °C and 500 °C are designated as TSB300 and TSB500, respectively. Apatite ore was sourced from Vietnam Apatite Ltd, located in Lao Cai Province, Vietnam (22°29′8.02″N, 103°

58′14.38″E). (22°29′8.02″N, 103°58′14.38″E).[30] The amendments (biochar and apatite) underwent pre-treatment by size reduction to a fraction less than 1 mm before being incorporated into the soil.[11]

2.2. Experimental design

For each treatment plot, 100 g of homogenized contaminated soil was carefully measured and transferred into individual glass containers. To prepare the experimental mixtures, biochar and apatite were added to the soil at predetermined mass ratios of 3%, 6%, and 10% biochar by weight. Additionally, the biochar–apatite combinations were prepared as follows: (i) a mixture of 3 g of biochar and 3 g of apatite was combined with 100 g of the studied soil to create a 3% combination sample, and (ii) a mixture containing 6 g of biochar and 6 g of apatite was blended with 100 g of the studied soil to create a 6% combination sample. These treatments were designed to investigate the effects of varying biochar and apatite application rates on the soil's properties.

The experiment included 10 treatment groups, each consisting of 3 replicates, totalling 30 soil samples that underwent incubation. Additionally, 3 blank soil replicates (untreated contaminated soil) were incorporated as controls, resulting in a total of 33 samples. The treatment groups varied in the application rates of biochar (TSB300 and TSB500) and apatite ore, with biochar derived from taro stalk (*Colocasia esculenta*), pyrolyzed at 300 °C (TSB300) or 500 °C (TSB500).

The incubation took place over 30 days under controlled laboratory conditions, with regular monitoring of soil moisture to maintain consistency. The glass containers were randomized within blocks to minimize potential environmental influences, such as light, humidity, and temperature fluctuations, which could affect the results. This randomization process ensured that the placement of the containers within the incubation space was unbiased and that any environmental gradients did not influence the treatment outcomes, thereby enhancing the reliability and validity of the results.[29] A detailed description of the incubation setup, including temperature conditions, is provided in Table 1.

The soil samples were incubated for 30 days within an ambient temperature range of 22–28 °C. To maintain a stable moisture content of approximately 70%, deionized water was gradually added to the soil every 48 hours, as described by Vuong *et al.* (2025).[18] Moisture levels were carefully controlled throughout the incubation, while temperature was monitored only within the typical laboratory range of 22–28 °C. Since temperature affects microbial activity, metal mobility, and sorption dynamics, variations in this range were deemed insignificant for the study's objectives. However, future research should consider precisely regulating and documenting temperature fluctuations to better understand their potential impact on metal speciation and biochar performance. After the 30-day incubation, the soil was dried in an oven at 45 °C for 48 hours, ground into a fine powder, and passed through a 2 mm sieve for further analysis. Sieving to <2 mm is a standard preparatory procedure, but further grinding to <1 mm may be necessary for specific heavy metal analyses.[29]

2.3. Analyzing soil properties and amendment characteristics

2.3.1. Characterization of physical and chemical properties. The physicochemical properties of the soil samples and amendments (biochar and apatite) were characterized at two-time points: before incubation and after one month of incubation with the amendments. To determine the pH and EC of the soil and amendments (TSB300, TSB500, and AP), a standardized 1 : 10 (w/v) ratio of sample to deionized water was used to prepare the measurement solutions. A Hanna HI 9124 pH meter was then employed to perform the analysis.[31] To characterize the texture of the investigated soil, the pipette method was employed to analyze the proportions of clay, silt, and sand particles within the soil sample.[32] An assessment of organic carbon (OC) in the soil samples and amendments (biochar and apatite) was conducted using the Walkley–Black titration method.[33]

2.3.2. Heavy metal analysis. Microwave-assisted acid digestion was employed as a pretreatment step to prepare the soil sample for subsequent analysis of total heavy metal

Table 1 The incubation experiment[a]

Sample	Sample code	Apatite (g)	Biochar (g)	Soil (g)	Ratio (biochar) (%)	Ratio (apatite) (%)
Contaminated soil (CS, untreated)	BS	0	0	100	0	
CS + 3% TSB300	TB3_3	0	3	100	3	N/A
CS + 6% TSB300	TB3_6	0	6	100	6	N/A
CS + 10% TSB300	TB3_10	0	10	100	10	N/A
CS + 3% TSB500	TB5_3	0	3	100	3	N/A
CS + 6% TSB500	TB5_6	0	6	100	6	N/A
CS + 10% TSB500	TB5_10	0	10	100	10	N/A
CS + 3% TSB300 + 3% AP	TB3A3	3	3	100	3	3
CS + 6% TSB300 + 6% AP	TB3A6	6	6	100	6	6
CS + 3% TSB500 + 3% AP	TB5A3	3	3	100	3	3
CS + 6% TSB500 + 6% AP	TB5A6	6	6	100	6	6

[a] TSB300: biochar derived from taro stalk (*Colocasia esculenta*) pyrolysis at a temperature of 300 °C. TSB500: biochar derived from taro stalk (*Colocasia esculenta*) pyrolysis at a temperature of 500 °C; BS: untreated soil sample contaminated with lead (Pb) and zinc (Zn) serving as a reference point for comparison without biochar amendment; incubation time: 30 days. N/A: not applicable.

concentrations. Microwave-assisted acid digestion was performed on the soil sample to prepare it for subsequent analysis. A 0.1000 g subsample of the soil was weighed and then mixed with 8 mL of a concentrated HNO_3 : HCl solution (1 : 3 v/v) in a Mars 6 microwave system.[27,30] The operating conditions employed during microwave digestion are presented in Table S1 of the ESI†. For the inductively coupled plasma mass spectrometry (ICP-MS) analysis performed using an Agilent 7900 instrument, the specific operational parameters are provided in Table S2 of the ESI†. Validation of the analytical method for Pb and Zn was achieved through the analysis of MESS-4, a certified reference material for sediment. The recoveries of these elements in MESS-4 were 109.27% for Pb, and 103.22% for Zn, as detailed in Table S2 of the ESI†. A five-step sequential extraction procedure derived from Tessier's method[12] was employed to determine the operational speciation of heavy metals within the soil samples (Table S3, ESI†). This method separates metals based on their extractability, defining five fractions: exchangeable (F1), carbonate-bound (F2), associated with Mn/Fe-hydroxides (F3), complexed with organic matter (F4), and residual (F5).

2.3.3. Surface characterization of amendments. Fourier transform infrared spectroscopy (FTIR) with a JASCO FT/IR-4600 instrument (JASCO International Co. Ltd, Tokyo, Japan) was utilized to investigate the surface chemistry of apatite and biochar (TSB300 and TSB600) by identifying the functional groups present.[30] To investigate the surface morphology and elemental composition of the amendments, high-resolution imaging and elemental analysis were performed using a field emission electron microscope (FE-SEM, JSM-6700F, JEOL, Akishima, Tokyo, Japan) coupled with an energy dispersive spectrometer (EDS).[10] Nitrogen gas adsorption–desorption isotherms were measured using a Brunauer–Emmett–Teller (BET) surface area analyzer (TriStar II 3020, Micromeritics Instrument Corporation, USA) to determine the surface area and pore size distribution of the materials.[10]

2.4. Statistical analysis

Statistical analyses and data visualizations were conducted using a range of software programs. Initial data manipulation and basic calculations were performed in Microsoft Excel 2019. For more advanced statistical analyses and the generation of high-quality graphs, Origin Pro 2021 (OriginLab Corp., USA) was used.

Triplicate data were statistically analyzed in Excel 2019 to calculate mean values and standard deviations (SD). All data presented in tables and figures are expressed as the mean ± SD. To assess potential differences between treatment means, a one-way analysis of variance (ANOVA) was conducted using Origin Pro 2021, assuming homogeneity of variances and normality of residuals. Statistical significance was determined at a level of $p < 0.05$.

Additionally, principal component analysis (PCA) and Spearman correlation analysis were carried out using Origin Pro 2021 to explore data patterns and relationships between variables. The Spearman correlation was chosen due to its non-parametric nature, making it suitable for the type of data typically encountered in soil research, particularly when evaluating correlations between soil characteristics and heavy metal concentrations.

3. Results and discussion

3.1. Evaluation of soil and amendment properties through physicochemical analyses

The initial soil pH, organic carbon (OC) content, and electrical conductivity (EC) are key factors that influence the mobility and bioavailability of heavy metals in the soil. An evaluation of the analyzed soil's fundamental physicochemical properties (pH, EC, and OC) was conducted, with the results presented in Table 2. The data reveal a moderate organic carbon content (average: 3.21 ± 0.23%) and an electrical conductivity (average: 44.8 ± 0.5 μS cm^{-1}) in the soil. The soil pH was determined to be 6.97. A neutral pH is generally linked to reduced metal adsorption, as it provides fewer metal-binding sites compared to acidic or alkaline soils, where such sites are more abundant. Furthermore, low organic carbon (OC) content, which plays a key role in metal binding *via* organic functional groups, may increase the mobility of contaminants. Reduced electrical conductivity (EC), which indicates a limited ion exchange capacity, can also prevent metal ions from binding, thus enhancing their mobility in the soil solution. By understanding these factors, soil

Table 2 Properties of the studied soil, biochar, and apatite ore[a]

Properties	Unit	Studied soil	TSB300	TSB500	AP
Sand	%	66.72 ± 0.43	—	—	—
Silt	%	6.32 ± 0.21	—	—	—
Clay	%	26.96 ± 0.54	—	—	—
pH		6.97 ± 0.01	10.08 ± 0.01	10.68 ± 0.01	9.06 ± 0.01
OC	%	3.21 ± 0.23	44.56 ± 0.25	45.32 ± 0.41	3.04 ± 0.09
EC	μS cm^{-1}	44.8 ± 0.8	4070 ± 2.5	3520 ± 3.5	370.6 ± 0.8
Pb	mg kg^{-1}	4165.1 ± 19.6	1.1 ± 0.4	1.2 ± 0.3	5.1 ± 0.6
Zn	mg kg^{-1}	3424.9 ± 20.4	2.8 ± 0.4	3.7 ± 0.5	9.5 ± 0.3
$S_{(BET)}$	m^2 g^{-1}	—	31.79	7.03	0.41

[a] OC: organic carbon; EC: electrical conductivity; TSB300: biochar derived from taro stalk (*Colocasia esculenta*) pyrolysis at a temperature of 300 °C; TSB500: biochar derived from taro stalk (*Colocasia esculenta*) pyrolysis at a temperature of 500 °C; AP: apatite ore; S(BET): surface area, LOD: limit of detection, –: no analysis; mean ± standard deviation; three replicates $n = 3$.

amendments such as biochar and apatite can be tailored to more effectively immobilize heavy metals, minimize their environmental impact, and promote soil health.

Furthermore, the analysis revealed significant heavy metal contamination, with average concentrations of Pb and Zn at 4165.1 ± 19.6 mg kg^{-1} and 3424.9 ± 20.4 mg kg^{-1}, respectively. These findings align with previous studies conducted in the same area, which reported elevated Pb and Zn levels ranging from 2000 to over 4000 mg kg^{-1} (ref. 11,27 and 30).

Notably, the measured heavy metal concentrations significantly exceed the permissible limits established by Vietnamese National Technical Regulation (QCVN 03-MT: 2015/BTNMT) for agricultural soils by factors of approximately 59.5 and 17.1 for Pb and Zn, respectively (permissible limits: Pb = 70 mg kg^{-1}, Zn = 200 mg kg^{-1}).[34]

Biochar and apatite ore were chosen for their ability to modify the physicochemical properties of the soil and reduce heavy metal contamination. While the soil's neutral pH (6.97) enhances the solubility and mobility of Pb and Zn,[35] biochar, with its large surface area, can increase organic carbon (OC) content, improve metal retention, and slightly raise pH, thereby reducing metal solubility. Apatite ore reacts with Pb and Zn to form insoluble phosphate complexes, reducing their mobility and bioavailability, particularly in neutral pH soils. With Pb (4165.1 ± 19.6 mg kg^{-1}) and Zn (3424.9 ± 20.4 mg kg^{-1}) levels being significantly high, both amendments were selected to immobilize these metals and decrease their environmental and health impacts. These amendments are especially effective for this soil, as they improve metal retention and mitigate

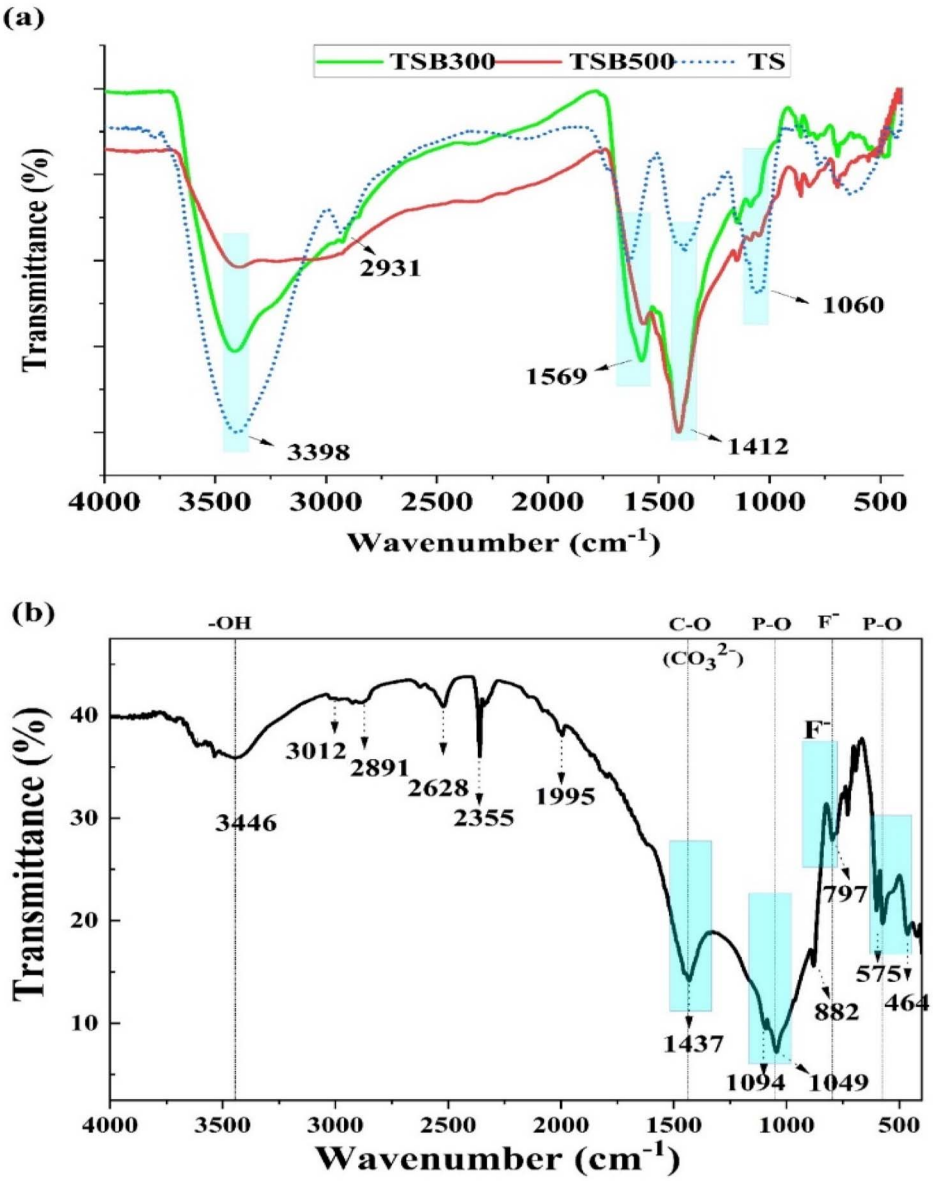

Fig. 1 FT-IR spectra of (a) the stem of the taro stalk (TS), biochar derived from the taro stalk's stem at 300 °C (TSB300), and at 500 °C (TSB500), and (b) apatite ore.

contamination risks by addressing its low OC, EC, and neutral pH.

3.2. Characteristics of amendments

3.2.1. Fourier Transform Infrared Spectroscopy analysis of amendments (FT-IR). Fig. 1 presents the FT-IR spectra of the stem of the taro stalk (TS), biochars derived from TS at 300 °C (TSB300) and 500 °C (TSB500), and apatite ore. Fig. 1a focuses on a comparison among TS, TSB300 and TSB500. All spectra exhibit a characteristic peak at about 3398 cm^{-1}, assigned to O–H stretching vibrations, with decreasing intensity in the order TS > TSB300 > TSB500.[36,37] This trend indicates a progressive decline in hydroxyl groups due to decomposition at higher pyrolysis temperatures. Additionally, a peak around 2931 cm^{-1}, attributed to C–H stretching,[38] was prominent in TS but diminished significantly in TSB300 and TSB500, signifying C–H group decomposition with increasing pyrolysis temperature. The peak at 1569 cm^{-1} corresponded to aromatic C=C stretching vibrations,[38,39] while peaks near 1412 cm^{-1} were likely due to phenolic –OH and C–O linkages.[40] These peaks were more intense in TSB300 and TSB500 compared to TS. The peak at 1060 cm^{-1}, assigned to C–O–H or C–O–C stretching,[36,41] was strongest in TS and negligible in TSB300 and TSB500.

The significant decrease in peak intensities of –OH (3398 cm^{-1}), C–H (2931 cm^{-1}), and C–O (1060 cm^{-1}) upon pyrolysis at 300 °C and 500 °C suggests the decomposition of cellulose, hemicellulose, and lignin components.[42] The FT-IR results of TSB300 and TSB500 primarily correspond to functional groups associated with cellulose (hydroxyl groups), hemicellulose (acetyl ester carbonyls), and lignin (carbonyl aldehydes).[18] The FT-IR spectrum of the apatite ore (Fig. 1b) displays four characteristic peaks at approximately 1094, 1049, 574, and 464 cm^{-1}. These peaks correspond to the signature vibrational modes of the PO_4^{3-} ion, assigned to the asymmetric stretching (1094 cm^{-1}), symmetric stretching (1049 cm^{-1}), asymmetric bending (574 cm^{-1}), and bending (464 cm^{-1}) of the P–O bond and O–P–O angle, respectively.[43,44] Additionally, peaks observed around 3618 and 3446 cm^{-1} were attributed to O–H stretching vibrations in hydroxyl groups (OH^-) or adsorbed water molecules.[30,45] The presence of a peak near 797 cm^{-1} confirms the incorporation of F^- ions into the apatite structure.

Furthermore, the presence of a CO_3^{2-} stretching vibration at 1437 cm^{-1} signifies that the analyzed ore sample is a fluoro-

Table 3 Key FT-IR peaks and corresponding functional groups of amendments

Peak (cm^{-1})	Functional group	Amendment	Significance/interaction
3398	O–H stretching vibrations	Taro stalk (TS), TSB300, TSB500	Indicates the presence of hydroxyl groups, potential for hydrogen bonding and adsorption of heavy metals
2931	C–H stretching	Taro stalk (TS)	Associated with alkyl groups, decreased in biochars, suggesting the loss of hydrophobicity with pyrolysis
1569	Aromatic C=C stretching vibrations	TSB300, TSB500	Indicates aromatic structures, relevant for π–π interactions with organic pollutants and metal ions
1412	Phenolic –OH and C–O linkages	TSB300, TSB500	Suggests the presence of phenolic groups, relevant for chelation or surface complexation with metals
1060	C–O–H or C–O–C stretching	Taro stalk (TS)	Indicates C–O groups; less significant in biochars, which could influence metal adsorption *via* surface interaction
1094, 1049	PO_4^{3-} asymmetric and symmetric stretching	Apatite ore	Characteristic of phosphate groups; important for precipitation or ion exchange with heavy metals
574, 464	PO_4^{3-} bending vibrations	Apatite ore	Associated with P–O bonds, key for adsorption mechanisms with heavy metals in soil solution
3618, 3446	O–H stretching vibrations	Apatite ore	Hydroxyl groups; potential for water molecule adsorption, influencing metal ion availability and interactions
797	F^- stretching vibration	Apatite ore	Indicates the incorporation of fluoride, relevant for ion exchange with metal ions
1437	CO_3^{2-} stretching vibration	Apatite ore	Indicates carbonate groups; important for complexation and adsorption of cations like Pb^{2+} and Zn^{2+}

hydroxycarbonate apatite, consistent with previous FT-IR studies of apatite ore.[45,46] These findings confirm the presence of key functional groups (PO_4^{3-}, OH^-, CO_2^{3-}) within the apatite ore structure, which have the potential to interact with heavy metals in soil solution *via* precipitation or ion exchange mechanisms as reported in the previous study.[30] The summary information of FT-IR peaks and Corresponding Functional Groups of Amendments is shown in Table 3.

3.2.2. SEM-EDS analysis of amendments. FE-SEM analysis of materials: a field emission electron microscope (FE-SEM) was employed to investigate the surface morphology of biochar (TSB300 and TSB500), and apatite ore (AP). The FE-SEM images depicting the surface morphology of TS, TSB300, and TSB500 are presented in Fig. 2.

FE-SEM micrographs demonstrate a clear distinction in surface morphology between elephant ear taro stem (TS) and apatite ore (AP) (Fig. 2a and d) compared to two kinds of biochar derived from TS at 300 °C (TSB300) and 500 °C (TSB500) (Fig. 2b and c). While TS and AP exhibited non-porous surfaces, TSB300 and TSB500 displayed a characteristically heterogeneous biochar structure with abundant pores.

During pyrolysis under anaerobic conditions, the decomposition of taro stem (TS) at 300 °C and 500 °C results in the release of gaseous species, including CH_4, H_2, CO, CO_2, which are byproducts of the process.[47] The evolution of these gases contributes to the formation of porosity and a honeycomb-like structure within the biochar. Scanning electron microscopy (SEM) images qualitatively confirm that the pore content in biochar produced at 300 °C (TSB300) and 500 °C (TSB500) is significantly higher compared to the raw taro stem (TS) and apatite ore (AP). Although a formal enumeration of the pores was not conducted in this study, the SEM images indicate a visible increase in porosity in TSB300 and TSB500, suggesting their greater potential for heavy metal adsorption compared to the native materials (TS and AP). This enhanced porosity likely contributes to their higher surface area, which is known to play a critical role in biochar's ability to adsorb contaminants. Studies have shown that a higher porosity provides more surface area for interaction with metal ions such as Pb and Zn, thus improving the biochar's adsorption capacity.[48] Biochar's microporous structure, formed during pyrolysis, creates more available adsorption sites, further increasing its capacity to retain heavy metals.[49]

Energy-dispersive X-ray spectroscopy (EDX) was used to analyze the elemental composition of the material surfaces, with the corresponding spectra shown in Fig. 3a–c.

The EDX results revealed that carbon (C) and oxygen (O) were the predominant elements in TSB300 and TSB500, as shown in Fig. 3a and b. In contrast, the apatite ore displayed a more diverse elemental profile, with trace amounts of calcium (Ca), potassium (K), iron (Fe), silicon (Si), magnesium (Mg), aluminum (Al), and others, along with the primary presence of C and O (Fig. 3c). These findings are consistent with prior research indicating that biochar, predominantly composed of carbon and oxygen, benefits from surface functional groups for heavy metal remediation.[50] Additionally, studies suggest that

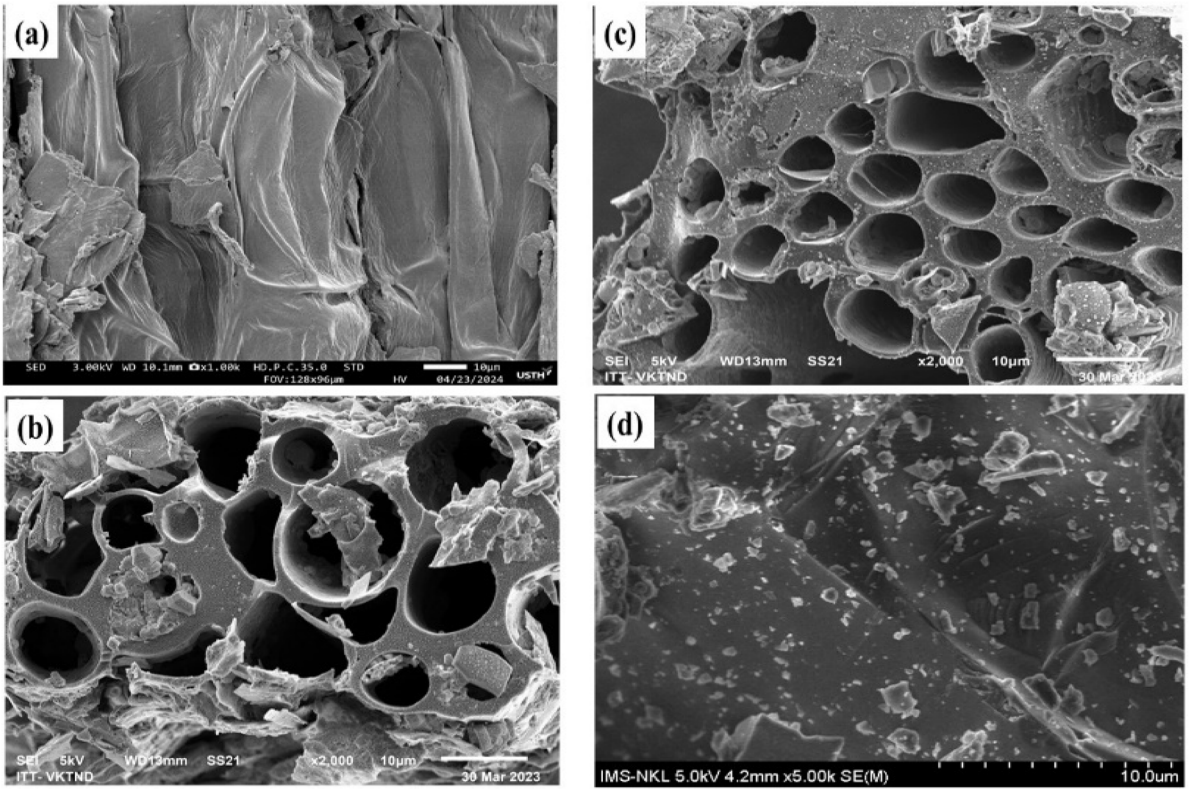

Fig. 2 Field emission electron microscope (FE-SEM) images of materials: (a) TS, (b) TSB300, (c) TSB500, (d) apatite (AP).

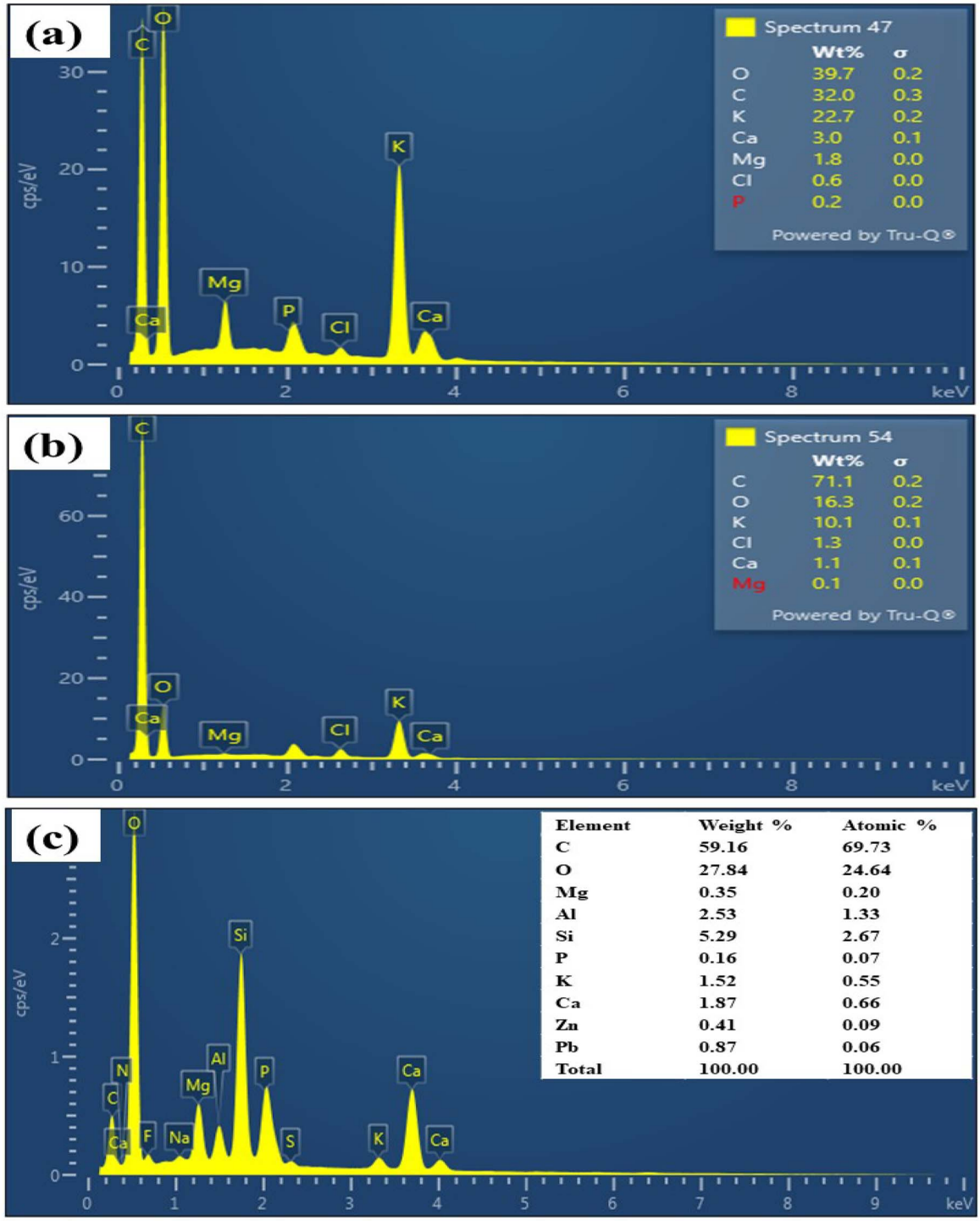

Fig. 3 Energy-dispersive X-ray spectroscopy (EDX) analysis of TSB300 (a), TSB500 (b), and apatite (c).

higher oxygen content on biochar surfaces improves the adsorption of divalent metals like Pb^{2+} and Zn^{2+}.[51] Apatite ore, classified as fluorine-apatite in the Lao Cai region, showed increased concentrations of silicon (Si), calcium (Ca), fluorine (F), and phosphorus (P), further distinguishing it from biochar.[10]

3.2.3. Brunauer–Emmett–Teller (BET) surface area analysis. BET surface area analysis, as detailed in Table 2, revealed a pronounced difference between biochar (TSB300 and TSB500) and apatite ore (AP). TSB300 exhibited a significantly higher surface area (31.79 $m^2 g^{-1}$) compared to AP (0.41 $m^2 g^{-1}$), which aligns with the general trend of increased surface area in biochar produced at higher temperatures. However, a surprising deviation from this trend was observed for TSB500. Despite being produced at a higher temperature (500 °C) compared to TSB300 (300 °C), TSB500 displayed a notably lower surface area

($7.03\ m^2\ g^{-1}$). This unexpected result can be explained by the decomposition of lignin functional groups at elevated temperatures (450–500 °C). The taro stems likely underwent more extensive thermal degradation of volatile organic compounds, which contributed to the reduction in porosity and surface area. This process results in a more condensed and less porous structure as the biomass undergoes further carbonization. This decomposition likely leads to pore shrinkage within the biochar structure, resulting in a decrease in the overall surface area of TSB500 compared to TSB300. This phenomenon of surface area reduction with increasing pyrolysis temperature has been documented in previous research conducted by Umchimia *et al.*, (2011),[47] who observed similar trends in biochar derived from cottonseed hulls pyrolyzed at different temperatures.

Biochar was selected for its substantial surface area, the presence of functional groups that facilitate metal adsorption, and its capacity to buffer soil pH. In soils with limited organic carbon (OC), biochar proves to be an effective amendment, enhancing metal retention and improving soil structure, which in turn diminishes the bioavailability and mobility of Pb and Zn. Conversely, apatite ore, although having a lower surface area than biochar, was chosen for its ability to form insoluble metal-phosphate complexes with Pb and Zn, thus reducing their bioavailability. Apatite also aids in buffering soil pH, making it especially useful in neutral to alkaline soils and providing a synergistic approach for immobilizing heavy metals in soils with low OC. The surface area of biochar and apatite significantly influences their efficiency in remediating Pb and Zn contamination. Biochar, with its larger surface area and higher pH, mainly utilizes adsorption and precipitation to immobilize metals, proving highly effective in reducing metal bioavailability. On the other hand, apatite, despite its smaller surface area, relies on precipitation and chemical interactions with metal ions to immobilize the metals, making surface area less critical. The combination of these materials offers a comprehensive solution for soil remediation by harnessing both adsorptive and precipitative mechanisms.

3.3. Soil pH, organic carbon (OC), and electrical conductivity (EC)

Soil properties such as pH, organic carbon (OC), and electrical conductivity (EC) are critical factors influencing the effectiveness of biochar in heavy metal remediation. The effects of biochar on these properties were significantly observed in the biochar-amended soils, as detailed in Table 4.

3.3.1. Soil pH. Soil pH plays a crucial role in determining the effectiveness of heavy metal remediation strategies, as it directly influences the exchangeable fractions of heavy metals in the soil matrix. As indicated in Table 4, all biochar-amended soils showed a significant increase in pH compared to the control (BS). ANOVA results revealed a statistically significant difference in pH across the various treatments ($p < 0.05$), and Tukey's post-hoc test further confirmed that biochar treatments led to a substantial increase in pH relative to the control ($p < 0.01$). The addition of TSB300 and TSB500 biochars caused a moderate elevation in soil pH after a one-month incubation period. Notably, a positive correlation was observed between the biochar amendment rate and the increase in soil pH. The TB5_10 treatment, which contained 10% TSB500 biochar, exhibited the highest pH (9.86), surpassing the TB3_10 treatment with 3% TSB300 biochar (9.67). These findings are consistent with previous studies,[10,11,18] which have shown that biochar generally has a higher pH compared to native soil. The elevated pH of biochar is likely a key factor in reducing the exchangeable forms of lead (Pb) and zinc (Zn) in the soils. An increase in pH facilitates the precipitation of Pb and Zn hydroxides, thereby decreasing the concentration of these metals in their exchangeable fraction (F1).

Table 4 Impact of biochar and apatite on soil organic carbon, electrical conductivity, and pH after one-month incubation[a]

Sample	pH	OC (mg kg^{-1})	EC (μS cm^{-1})
BS	6.98 ± 0.01^{h}	20.16 ± 0.46^{f}	44.8 ± 1.3^{k}
TB3_3	8.59 ± 0.01^{g}	39.54 ± 0.57^{e}	125.3 ± 0.4^{h}
TB3_6	9.08 ± 0.01^{f}	51.3 ± 0.62^{cd}	277.5 ± 0.5^{c}
TB3_10	9.67 ± 0.01^{b}	89.06 ± 0.64^{a}	459.9 ± 0.9^{a}
TB3A3	9.17 ± 0.01^{e}	40.59 ± 0.74^{e}	129.9 ± 0.8^{g}
TB3A6	9.39 ± 0.01^{d}	53.29 ± 0.89^{b}	191.0 ± 1.5^{i}
TB5_3	9.06 ± 0.01^{f}	39.54 ± 0.92^{e}	131.1 ± 1.3^{g}
TB5_6	9.17 ± 0.01^{e}	49.6 ± 0.56^{d}	183.9 ± 0.9^{e}
TB5_10	9.86 ± 0.01^{a}	87.24 ± 0.51^{a}	449.0 ± 1.5^{b}
TB5A3	9.16 ± 0.01^{e}	38.9 ± 0.54^{e}	$136.3 \pm 0.8f$
TB5A6	9.49 ± 0.01^{c}	52.71 ± 0.69^{bc}	252.7 ± 1.4^{d}

[a] Superscript letters throughout the text signify the absence of statistically significant differences ($p \geq 0.05$) between the compared groups based on student's *t*-test analysis.

In conclusion, biochar amendment significantly increases soil pH, enhancing the immobilization of lead (Pb) and zinc (Zn) by reducing their exchangeable fractions.

3.3.2. Organic carbon (OC). As shown in Table 3, biochar amendment significantly elevated soil organic carbon (OC) content compared to the control soil (BS) after a 30-day incubation period ($p < 0.05$). This observation aligns with the inherent carbon-rich nature of biochar. Furthermore, a positive correlation was observed between the biochar amendment rate and the resulting soil OC content. The TB3_10 treatment, containing 10% TSB300 biochar, exhibited the highest recorded OC value (89.06 ± 0.64 mg kg^{-1}), exceeding the TB5_10 treatment (87.24 ± 0.51 mg kg^{-1}) amended with the same 10% of TSB500 biochar. Consequently, the TB3_10 and TB5_10 samples displayed a substantial increase in OC content, with values 4.42 and 4.32 times higher, respectively, compared to the control. This gradual increase in soil OC content followed a dose-dependent pattern, with the order being 3% < 6% < 10% biochar amendment. The high OC content in the TB3_10 and TB5_10 samples can be attributed to the inherent OC content of the biochars themselves, with TSB300 (44.56 ± 0.25 mg kg^{-1}) displaying a slightly higher value compared to TSB500 (45.32 ± 0.41 mg kg^{-1}) as shown in Table 2. This finding corroborates previous research that has documented a positive association between biochar amendment rate and increased soil OC.[30,52,53]

This increase in OC content is attributed to the carbon-rich nature of biochar, which can interact with heavy metals like

Pb and Zn through functional groups such as carboxyl and phenolic groups. These interactions enhance metal immobilization, decreasing the metals' bioavailability and limiting their mobility.[54] Biochar thus plays a critical role in the sequestration of heavy metals in contaminated soils.

3.3.3. Electrical conductivity (EC). Electrical conductivity (EC) plays a significant role in soil research and remediation strategies for heavy metals. Table 4 presents the EC values of control and biochar-amended soils. The data reveals a statistically significant difference ($p < 0.05$) between the control soil and all incubated samples. Notably, the TB3_10 treatment, containing 10% TSB300 biochar, exhibited the highest EC value (459.9 ± 0.9 μS cm^{-1}). This value slightly exceeded that of the TB5_10 treatment (449.0 ± 1.5 μS cm^{-1}) with the same amendment rate, but different biochar (TSB500). This can be attributed to the slightly higher EC value of TSB300 (4070 ± 2.5 μS cm^{-1}) compared to that of TSB500 (3520 ± 3.5 μS cm^{-1}). This observation aligns with the inherent property of biochars to possess high EC, as evidenced by Table 4, which demonstrates their considerably higher values compared to native soil and apatite ore. These findings support previous studies that reported the positive correlation between biochar amendment rates and increased soil EC.[9,10]

Elevated EC can enhance the soil's ability to adsorb and immobilize heavy metals. However, high EC may also lead to competition for adsorption sites between metal ions and other cations like Ca^{2+} and Mg^{2+}, potentially reducing the efficiency of metal immobilization. It is important to monitor EC levels to avoid negative effects such as osmotic stress, nutrient imbalances, and soil salinization, which could compromise the long-term effectiveness of biochar in soil remediation.

In summary, biochar and apatite amendments resulted in increased soil pH, organic carbon, and electrical conductivity, all of which play essential roles in immobilizing heavy metals in contaminated soils. However, careful management of these properties is necessary to ensure the long-term success of biochar as a remediation tool, as excessively high pH or EC could have detrimental effects on soil health and nutrient availability.

3.4. Chemical speciation of lead and zinc in control and incubated soils after a 30-day incubation

3.4.1. Pb speciation. The chemical speciation of lead (Pb) in the control soil (BS) and incubated soils is presented in Table 5. This table details the distribution of Pb into various chemical fractions. For both Pb and Zn, a broader perspective of their chemical fraction distribution within the soil is illustrated in Table S4 (ESI)† and Fig. 4. Table S4† provides the percentage values for the chemical fractions (F1, F2, F3, F4, and F5) of Pb and Zn, presented as percentages, in both the control soil samples and those treated with biochar and apatite ore. Fig. 4a and b display the distribution of the chemical fractions for Pb (Fig. 4a) and Zn (Fig. 4b) in the form of 100% stacked bar charts. One-way ANOVA was used for statistical analysis to assess the mean concentrations of Pb and Zn across various treatments

Table 5 Chemical fractions of lead and zinc in soil after one-month incubation with biochar and apatite[a]

Sample	F1 (mg kg^{-1})	F2 (mg kg^{-1})	F3 (mg kg^{-1})	F4 (mg kg^{-1})	F5 (mg kg^{-1})
Pb					
BS	433.2 ± 13.2^{a}	2012.3 ± 45.2^{a}	700.2 ± 10.3^{a}	$182.0 \pm 4.9e$	837.3 ± 16.3^{cd}
TB3_3	287.7 ± 9.8^{c}	1970.9 ± 36.2^{a}	663.7 ± 11.1^{b}	277.1 ± 5.0^{a}	890.1 ± 22.8^{b}
TB3_6	211.62 ± 14.2^{de}	1756.6 ± 45.3^{c}	601.2 ± 11.6^{d}	226.5 ± 4.2^{c}	884.0 ± 20.5^{b}
TB3_10	121.8 ± 8.1^{f}	1961.3 ± 43.4^{a}	570.6 ± 9.8^{e}	213.7 ± 5.3^{d}	893.1 ± 23.1^{b}
TB3A3	302.9 ± 9.1^{c}	1963.6 ± 53.2^{a}	657.6 ± 12.4^{b}	254.9 ± 3.2^{b}	886.7 ± 19.8^{b}
TB3A6	211.6 ± 8.0^{e}	1898.7 ± 36.2^{b}	598.22 ± 10.7^{d}	218.6 ± 4.5^{d}	749.7 ± 14.2^{e}
TB5_3	347.1 ± 10.7^{b}	1987.9 ± 34.8^{a}	575.4 ± 8.6^{e}	232.3 ± 6.9^{c}	851.2 ± 18.6^{bc}
TB5_6	216.2 ± 11.8^{de}	1866.2 ± 28.5^{b}	619.5 ± 9.5^{cd}	216.4 ± 3.6^{d}	791.6 ± 28.3^{de}
TB5_10	141.6 ± 10.9^{f}	1716.5 ± 42.1^{c}	572.3 ± 8.4^{e}	210.4 ± 5.9^{d}	1027.5 ± 30.1^{a}
TB5A3	231.4 ± 9.8^{d}	1927.0 ± 53.1^{a}	639.3 ± 10.3^{bc}	217.1 ± 5.5^{d}	799.2 ± 24.4^{de}
TB5A6	222.3 ± 15.3^{de}	1871.3 ± 64.2^{b}	599.7 ± 14.9^{d}	212.5 ± 4.0^{d}	761.1 ± 30.3^{e}
Zn					
BS	317.0 ± 11.1^{a}	613.8 ± 10.5^{bc}	1053.9 ± 40.6^{a}	96.2 ± 2.3^{f}	1344.0 ± 23.7^{a}
TB3_3	160.5 ± 10.2^{dc}	474.3 ± 11.6^{e}	1057.3 ± 50.2^{a}	121.7 ± 1.3^{c}	1238.2 ± 12.2^{b}
TB3_6	137.1 ± 12.2^{ef}	593.3 ± 12.8^{d}	986.7 ± 26.4^{b}	120.3 ± 3.3^{c}	1117.0 ± 15.3^{c}
TB3_10	129.4 ± 10.6^{f}	576.9 ± 11.4^{d}	981.5 ± 30.4^{b}	115.9 ± 2.5^{d}	1242.9 ± 21.7^{b}
TB3A3	150.8 ± 11.3^{de}	642.1 ± 12.5^{b}	1061.9 ± 30.6^{a}	148.2 ± 2.9^{b}	1324.9 ± 19.3^{a}
TB3A6	$137,3 \pm 9.1^{ef}$	569.3 ± 13.4^{d}	995.9 ± 28.2^{b}	124.1 ± 3.2^{c}	1066.5 ± 16.5^{d}
TB5_3	172.7 ± 10.3^{c}	646.8 ± 10.3^{b}	993.6 ± 29.6^{b}	108.5 ± 1.9^{e}	1396.5 ± 20.1^{a}
TB5_6	160.5 ± 12.4^{dc}	561.2 ± 12.5^{d}	1056.1 ± 21.4^{a}	127.0 ± 4.2^{c}	1287.5 ± 16.0^{b}
TB5_10	205.9 ± 12.8^{b}	663.0 ± 12.8^{b}	1052.9 ± 30.6^{a}	155.5 ± 1.3^{a}	1357 ± 18.4^{a}
TB5A3	164.8 ± 10.1^{dc}	752.5 ± 21.9^{a}	1045.8 ± 31.8^{a}	115.7 ± 2.6^{d}	1144.1 ± 23.4^{c}
TB5A6	187.7 ± 8.0^{bc}	623.7 ± 20.2^{bc}	1016.9 ± 22.5^{a}	112.6 ± 4.5^{d}	1166.3 ± 13.9^{c}

[a] Superscript letters throughout the text signify the absence of statistically significant differences ($p \geq 0.05$) between the compared groups based on student's *t*-test analysis. F1: exchangeable fraction; F2: carbonate fraction; F3: Fe/Mn-oxide fraction; F4: organic carbon fraction; F5: residual fraction.

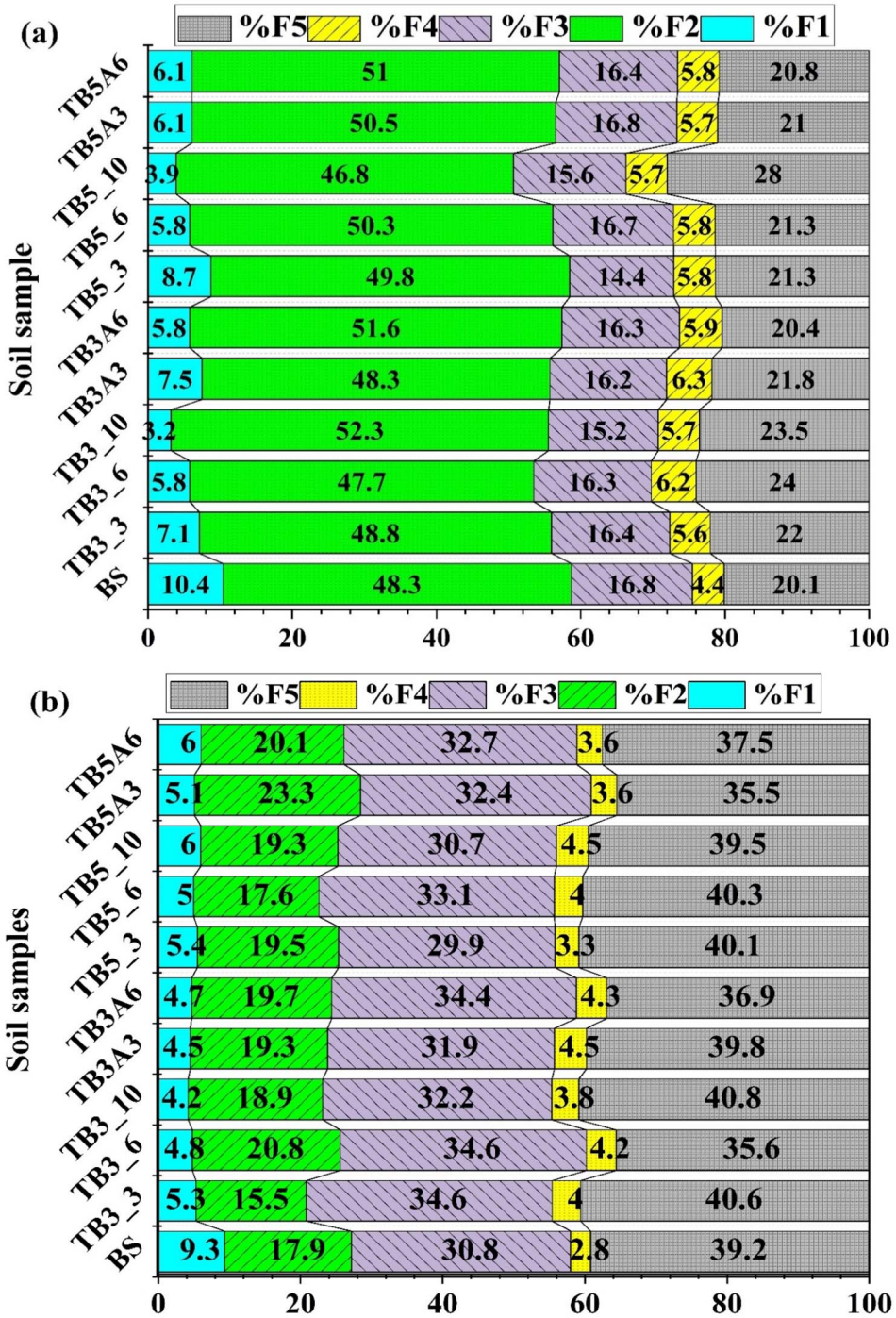

Fig. 4 Percentage of Pb (A) and Zn (B) chemical fractions in studied soils after 30 days of incubation with biochar and apatite.

(biochar, apatite ore, control). A p-value below 0.05 was regarded as statistically significant. Tukey's HSD post-hoc test indicated that the biochar treatment led to a significant reduction in the bioavailable Pb fraction (F1) relative to the control ($p < 0.05$).

Fig. 4 and Table S4† reveal that the control soil sample (BS) exhibited a decreasing order of Pb concentration distribution: F2 (48.3%) > F5 (20.1%) > F3 (16.8%) > F1 (10.4%) > F4 (4.4%). Pb was predominantly present in the carbonate-bound form (F2) and least in the organic carbon-bound form (F4) and exchangeable form (F1). The distribution pattern of Pb across the different forms underwent alterations upon incubation with varying biochar and apatite ratios in the soil.

3.4.1.1. Exchangeable fraction (F1_Pb). Sequential extraction revealed a significant decrease in the exchangeable Pb (F1_Pb) fraction in biochar-amended soil samples compared to the control soil (BS). The F1_Pb content in BS was 433.2 ± 13.2 mg kg^{-1}, contributing to 10% of the total Pb in the studied soil's five chemical fractions. In contrast, biochar-amended soils

exhibited values ranging from 3.2% to 9%. Notably, the lowest F1_Pb concentration was observed in sample TB3_10 (121.8 ± 8.1 mg kg^{-1}), contributing to 3.2%, when the soil was amended with 10% TSB300 biochar. This result indicates that the exchangeable fraction of Pb decreased by up to 71.8% compared to the control soil (BS). This trend continued with sample TB5_10 (3.9%), amended with 10% TSB500 biochar. Statistical analysis ($p < 0.05$) confirmed a significant reduction in F1_Pb across all biochar amendment ratios (3%, 6%, and 10%) and co-amendment ratios (3 : 3% and 6 : 6% biochar–apatite) compared to the control. These findings demonstrate a substantial alteration in Pb mobility upon biochar amendment, suggesting its potential for Pb immobilization in contaminated soils. This result demonstrates the effectiveness of biochar and apatite amendment in reducing the exchangeable Pb fraction (F1_Pb) within the amended soil samples. Notably, a dose-dependent decrease in F1_Pb was observed, with higher biochar amendment rates leading to a further reduction in exchangeable Pb. This suggests a reduction in Pb mobility within the soil matrix, thereby mitigating the risk of Pb leaching and subsequent environmental contamination. These results align with previous studies, which reported a significant decrease in soil F1_Pb following biochar amendment at appropriate ratios.[11,29,55] However, our study extends these findings by highlighting the dose-dependent reduction of F1_Pb, with the most substantial decrease (71.8%) observed at a 10% biochar amendment. Moreover, the biochar used in our research, derived from taro stems, may exhibit different properties compared to biochar from other feedstocks used in similar studies. This variability in biomass origin could influence the biochar's ability to immobilize Pb, as biochar properties such as cation-exchange capacity, surface functional groups, and Pb interaction capabilities are known to vary based on feedstock.[10,29]

The decrease in exchangeable Pb (F1_Pb) following biochar and apatite amendment can be attributed to several mechanisms. Biochar raises soil pH, promoting lead precipitation as $Pb(OH)_2$ and lead carbonate complexes, thereby reducing its bioavailability.[56] Biochar also contains functional groups (*e.g.*, carboxyl, hydroxyl) that form complexes with lead, further immobilizing it.[56] Additionally, the oxidation of biochar enhances its ability to adsorb lead. Co-amendment with apatite facilitates the precipitation of lead phosphate minerals, such as Pb5(PO4)3X, which are less soluble and bioavailable,[10] thus reducing lead mobility and toxicity.[57]

3.4.1.2. Carbonate fraction (F2_Pb). The sequential extraction results indicate that lead (Pb) predominantly resides in the carbonate-bound fraction (F2), which represents approximately 50% of the total Pb across all fractions in the soil samples (Fig. 4a). In the control soil (BS), the F2 fraction accounted for 48.3% of the total Pb, establishing a baseline for understanding Pb speciation in the soil. The carbonate-bound fraction typically represents Pb that is loosely associated with soil minerals, often in the form of carbonates and is, therefore, more susceptible to mobilization under changing soil conditions, such as variations in pH or the presence of competing ions. Biochar amendment, in combination with apatite, was expected to influence Pb immobilization within the carbonate-bound fraction, given biochar's known capacity to alter soil pH, enhance metal adsorption, and potentially promote metal precipitation. However, the results from this study revealed that the application of biochar at various ratios (3%, 6%, and 10%) alone, as well as co-amendment with apatite (3% and 6%), did not result in statistically significant changes in the F2_Pb fraction compared to the control ($p > 0.05$). This suggests that, at the applied amendment levels and under the experimental conditions used (30-day incubation), the biochar–apatite treatment had a minimal effect on the Pb speciation in the carbonate-bound fraction.

Notably, while the general trend across all biochar and co-amended treatments was non-significant, the TB3_10 sample (which consisted of 10% biochar) showed a significant outlier with an F2 content of 52.3%. This indicates that, in this specific treatment, there was a slight but notable increase in the proportion of Pb in the carbonate-bound fraction. This outlier may reflect an enhanced ability of biochar at higher concentrations (10%) to either promote the precipitation of Pb-carbonate complexes or alter soil pH in a manner that stabilizes Pb in the carbonate-bound fraction. The increase observed in TB3_10 suggests that biochar application at higher ratios may facilitate the formation of more stable Pb-carbonate complexes, though this effect was not consistently observed across other treatments.

The results suggest that biochar and apatite amendments have a minimal impact on Pb immobilization in the carbonate fraction, especially at the applied amendment rates over a 30-day incubation period. The short incubation time may not have been sufficient for the amendments to fully alter Pb speciation, and the control soil's high carbonate-bound Pb could limit the effects of biochar and apatite. This finding is consistent with previous studies, such as Dang *et al.* (2019)[11] and Nguyen *et al.* (2024),[10] which also observed limited changes in Pb in the carbonate fraction, likely due to biochar's moderate influence on soil pH and its weaker affinity for Pb compared to other fractions like iron/manganese oxides or organic matter.

Overall, these findings suggest that while biochar and apatite can influence Pb mobility and bioavailability, their effect on Pb in the carbonate-bound fraction may be limited, especially in the conditions of this study. Further research is needed to assess the impact of higher biochar concentrations, longer incubation periods, and varying biochar properties on Pb immobilization, particularly in different soil types and environmental conditions.

3.4.1.3. Fe/Mn-oxide fraction (F3_Pb). The sequential extraction results reveal that the Fe/Mn-oxide-bound fraction (F3) in the control soil (BS) contained an initial concentration of lead (Pb) of 700.2 ± 10.3 mg kg^{-1}, which accounted for approximately 17% of the total Pb (Fig. 4a and Table S4†). This fraction typically represents Pb that is adsorbed or bound to iron and manganese oxides in the soil. Pb in this fraction is considered relatively stable and less bioavailable than the exchangeable or carbonate-bound fractions, as it is more tightly bound to soil minerals. However, despite its relative stability, Pb in the F3 fraction may still be subject to mobilization under

conditions that favour the reduction of metal oxides or changes in soil chemistry. Therefore, the ability to alter Pb speciation in this fraction has significant implications for the long-term stabilization and immobilization of Pb in contaminated soils.

Upon biochar amendment, the F3_Pb concentration was significantly reduced ($p < 0.05$) across all amended soil samples compared to the control after a 30-day incubation period. This reduction suggests that biochar addition can effectively influence Pb speciation in the Fe/Mn-oxide-bound fraction, likely through a combination of mechanisms including changes in pH, surface area expansion, and enhanced adsorption capacity of biochar. Biochar is known for its high surface area and porous structure, which can facilitate the adsorption of metals like Pb, thereby reducing the mobility of these contaminants in soil. Additionally, biochar's ability to increase soil pH may contribute to the destabilization of metal oxides, promoting the desorption of Pb from the iron and manganese oxides and potentially shifting it to more stable fractions.

Interestingly, the proportion of Pb in the F3 fraction was similar between soils amended with TSB300 biochar (3% amendment rate) and those amended with a higher rate of TSB500 biochar (6% amendment rate). This finding suggests that the impact of biochar on Pb stabilization in the F3 fraction may reach a threshold beyond which additional biochar application does not significantly alter the proportion of Pb bound to Fe/Mn oxides. The lack of a substantial difference in F3_Pb between the two biochar amendment rates could indicate that a certain amount of biochar may be sufficient to saturate the available binding sites for Pb in the Fe/Mn-oxide fraction, beyond which additional biochar does not further enhance Pb immobilization within this fraction. This outcome aligns with the idea that, while biochar can significantly influence the distribution of Pb across various fractions, the effects may plateau at higher biochar amendment rates for specific metal species, such as Pb.

The significant reduction in F3_Pb after biochar amendment highlights its potential to immobilize Pb in soils by shifting it to less mobile, more stable fractions. This decreases the likelihood of Pb leaching into groundwater or being absorbed by plants, reducing environmental risks, especially in Pb-contaminated areas. Previous studies have shown that biochar's porous structure and high surface area help stabilize Pb in less bioavailable forms, likely through pH modification and enhanced metal adsorption.[58,59]

The results also suggest that biochar–apatite co-amendments could further enhance Pb immobilization, driving Pb into more stable forms in the Fe/Mn-oxide fraction, which is less prone to leaching. In conclusion, biochar effectively reduces Pb in the F3 fraction, offering a potential strategy for mitigating Pb contamination in soil and water. Further research is needed to assess the long-term stability of Pb and explore interactions with other amendments like apatite.

3.4.1.4. Organic carbon fraction (F4_Pb). The organic-bound fraction (F4) is typically characterized by heavy metals that are adsorbed or bound to organic matter in the soil. These metals are considered less bioavailable compared to those in the exchangeable or carbonate-bound fractions, as they are often tightly associated with soil organic matter, which can limit their mobility and potential for plant uptake. In this study, the control soil (BS) exhibited a relatively low Pb concentration in the F4 fraction, with approximately 4% of the total Pb content residing in this organic-bound form (Fig. 4a). This low proportion suggests that, under normal soil conditions, Pb is predominantly associated with more mobile or readily exchangeable forms, such as those bound to carbonates or iron/manganese oxides, rather than with organic matter.

Upon biochar and biochar–apatite co-amendment, a slight but statistically significant ($p < 0.05$) increase in the proportion of Pb in the F4 fraction was observed, particularly in soils amended with TSB500 biochar at the 10% rate and those amended with 3% and 6% biochar–apatite ratios. The proportion of Pb in the F4 fraction ranged from 5.6% to 6.3% in these co-amended soils, compared to the 4% observed in the control (Fig. 4a). This increase, while modest, suggests that biochar–apatite co-amendment may influence the speciation of Pb by promoting its association with organic matter in the soil, thereby enhancing its stabilization in a less mobile, organic-bound form.

The observed increase in the F4_Pb proportion can be attributed to several mechanisms associated with biochar's role in soil chemistry. Biochar is known for its large surface area and porosity, which can provide numerous binding sites for heavy metals, including Pb. Moreover, biochar's capacity to modify soil pH, typically raising it, could lead to changes in the solubility and speciation of Pb, promoting its adsorption onto soil organic matter. This pH-driven process could encourage Pb to bind more readily to organic compounds, resulting in an increased proportion of Pb in the organic-bound fraction (F4). Additionally, biochar's presence may enhance the formation of metal–organic complexes, further stabilizing Pb in the soil matrix.

The addition of apatite to the biochar co-amendment likely contributes to the observed shift in Pb speciation toward the organic-bound fraction. Apatite promotes Pb precipitation through metal-phosphate complex formation, while biochar helps retain Pb on organic surfaces, enhancing its stabilization in less bioavailable forms. This synergistic effect may reduce Pb mobility and bioavailability, making it less prone to leaching and plant uptake.

The increase in F4_Pb, although modest, is significant for mitigating environmental risks, as Pb in this fraction is less bioavailable and less likely to leach into groundwater. These findings align with previous studies that show biochar enhances metal retention in the organic-bound fraction, highlighting its role in long-term Pb immobilization.[10,18] In conclusion, biochar–apatite co-amendment effectively stabilizes Pb in a less mobile form, offering a promising strategy for managing Pb-contaminated soils. Further research is needed to explore the mechanisms behind Pb binding in the organic fraction and evaluate the long-term stability of Pb and other heavy metals in this form.

3.4.1.5. Residual fraction (F5_Pb). The residual fraction of Pb (F5_Pb) in the control soil (BS) was 837.3 ± 16.3 mg kg^{-1}, representing approximately 20.1% of the total Pb. This fraction,

considered the most stable and least bioavailable, serves as an important indicator of the long-term immobilization of Pb within the soil matrix. Interestingly, the biochar–apatite co-amendment significantly increased ($p < 0.05$) the proportion of F5_Pb in most treated soils when compared to the control. This increase suggests that biochar, in combination with apatite, can effectively enhance the sequestration of Pb in a more stable, less mobile form, potentially reducing its bioavailability and toxicity in the soil environment. However, it is worth noting that for the TB3A6 and TB5A6 treatments, the increase in F5_Pb was not statistically significant, indicating that the biochar–apatite co-amendment's effectiveness in promoting Pb stabilization may be influenced by specific treatment concentrations or other soil conditions, such as pH or organic matter content, which could affect the availability and reactivity of Pb.

The proportion of F5_Pb across the co-amended soils ranged from 20.4% to 28.0%, reflecting a substantial increase compared to the control. These findings suggest that the biochar–apatite co-amendment may drive the transformation of Pb from more labile fractions, such as F1 (exchangeable fraction) and F3 (carbonates), into less reactive and more stable fractions, such as F4 (Fe/Mn oxides) and F5 (residual). This shift could potentially reduce the mobility of Pb, preventing its uptake by plants and minimizing its availability to soil microorganisms, thereby decreasing the overall environmental risk posed by Pb contamination. The increased proportion of F5_Pb in the co-amended soils aligns with prior studies, which have consistently reported a similar trend of reduced F1 and increased F5 following biochar amendment in contaminated soils.[10,18] This transformation is likely facilitated by the interactions between biochar's surface functional groups and Pb, as well as the ability of apatite to promote phosphate-induced precipitation, leading to the incorporation of Pb into less mobile forms.

Further research is necessary to better understand the underlying mechanisms driving this transformation of Pb fractions in biochar–apatite co-amended soils. Factors such as the physicochemical properties of the biochar (*e.g.*, surface area, pH, and functional groups) and the dissolution rate of apatite may play key roles in mediating these changes. Additionally, the relative effectiveness of different biochar feedstocks and apatite sources in stabilizing Pb should be explored, as variations in these materials could influence the extent to which Pb is converted into more stable forms. Overall, the biochar–apatite co-amendment appears to offer a promising approach for enhancing the long-term immobilization of Pb in contaminated soils, thereby mitigating the risks associated with Pb contamination while promoting soil health.

3.4.1.6. Key findings on Pb speciation. (1) Exchangeable fraction (F1_Pb):

Biochar amendment significantly reduced the exchangeable Pb (F1_Pb) fraction, with the most notable decrease (71.8%) at 10% biochar amendment (TB3_10). The F1_Pb fraction decreased from 433.2 mg kg^{-1} in the control to as low as 121.8 mg kg^{-1} in the biochar-amended soil.

This suggests that biochar significantly reduces Pb mobility, thereby mitigating the risk of Pb leaching and environmental contamination.

(2) Carbonate fraction (F2_Pb):

Pb was predominantly found in the carbonate-bound fraction (F2), accounting for about 48.3% of total Pb in the control soil. Biochar and apatite amendment did not significantly alter the F2 fraction, with a minor outlier observed in the 10% biochar treatment (52.3%).

These findings suggest that biochar and apatite have a limited effect on Pb immobilization in the carbonate fraction during the study period.

(3) Fe/Mn-oxide fraction (F3_Pb):

Biochar amendment significantly reduced Pb in the Fe/Mn-oxide fraction (F3), with all treated soils showing a decrease in F3_Pb compared to the control ($p < 0.05$). The decrease was similar across different biochar treatments.

This indicates that biochar has the potential to immobilize Pb in this fraction, enhancing its stability.

(4) Organic carbon fraction (F4_Pb):

The organic-bound Pb fraction (F4) was relatively low in the control soil (~4%) and showed a slight, statistically significant increase (5.6% to 6.3%) in biochar–apatite co-amended soils.

The increase in F4_Pb suggests that biochar–apatite co-amendment may influence Pb speciation, potentially enhancing Pb retention in organic forms.

(5) Residual fraction (F5_Pb):

The residual Pb fraction (F5_Pb) in the control soil was 20.1% of total Pb. Biochar–apatite co-amendment significantly increased F5_Pb (20.4% to 28.0%) in most treated soils, indicating a shift of Pb into more stable, less bioavailable forms.

This suggests that biochar–apatite co-amendment can promote the transformation of Pb from more labile fractions (F1, F3) to more recalcitrant ones (F4, F5), which is beneficial for long-term Pb immobilization.

3.4.2. Zn speciation. Analysis of Zn speciation in the soil samples *via* sequential extraction revealed a specific order of fractions, with F5 being the most abundant, followed by F3, F2, F1, and F4 (F5 > F3 > F2 > F1 > F4). The impact of biochar amendment on Zn speciation was statistically variable ($p < 0.05$) across the samples when applied at different rates.

3.4.2.1. Exchangeable fraction (F1_Zn). Sequential extraction revealed that the control soil (BS) exhibited an exchangeable zinc (F1_Zn) fraction concentration of 317.0 ± 11.1 mg kg^{-1}, which accounted for approximately 9.3% of the total zinc content in the soil (Fig. 4b and Table S4 (ESI)†). This exchangeable zinc fraction is often considered the most mobile and bioavailable form of zinc, as it is readily exchangeable with soil solution and thus available for plant uptake or potential leaching into groundwater. The relatively high concentration of exchangeable Zn in the control sample indicates that the soil had a significant pool of zinc in this mobile form, which could pose a risk of environmental contamination if left unremediated.

Upon biochar–apatite co-amendment, a significant reduction in the F1_Zn fraction was observed compared to the control soil ($p < 0.05$), indicating that biochar–apatite interactions

effectively reduced the mobility of zinc in the amended soils. Specifically, the proportion of exchangeable zinc in co-amended soils ranged from 4.2% to 6.0%, with the most substantial reduction in the TB3_10 sample, where the exchangeable Zn concentration dropped to 121.8 ± 8.1 mg kg^{-1}, representing a decrease of up to 61.5% relative to the control. This significant reduction suggests that the biochar–apatite co-amendment strategy plays a crucial role in immobilizing zinc, thus limiting its bioavailability and potential for leaching into the surrounding environment.

The reduction in F1_Zn following biochar-amendment highlights its potential to modify the speciation and mobility of heavy metals. Biochar likely stabilizes zinc by increasing soil pH, providing surface area for adsorption, and promoting binding to soil minerals, reducing its presence in the exchangeable, more mobile form. The inclusion of apatite further enhances this effect, facilitating the formation of stable zinc-phosphate complexes that are less soluble and bioavailable.

These findings are consistent with previous studies showing that biochar reduces zinc bioavailability through mechanisms like adsorption and pH modification.[10,60] Notably, the combination of biochar and apatite was more effective in reducing exchangeable zinc (F1_Zn) than biochar alone, with higher biochar doses (10% in TB3_10) yielding a more pronounced effect.[10,18] This suggests a dose-dependent relationship, where increased biochar improves zinc immobilization by providing more surface area.

In conclusion, biochar–apatite co-amendments reduce zinc mobility and bioavailability, offering a promising strategy for mitigating zinc contamination in soils. Further research on their long-term effectiveness and impact on soil health is needed to optimize their use in remediation efforts.

3.4.2.2. Carbonate-bound fraction (F2_Zn). Sequential extraction analysis revealed that the carbonate-bound zinc (F2_Zn) fraction in the control soil (BS) had a concentration of 1053.9 ± 40.6 mg kg^{-1}, accounting for approximately 31% of the total zinc in the soil (Table S4†). Upon biochar–apatite co-amendment, the effects on the F2_Zn fraction were variable across the co-amended soil samples. In most cases, the proportion of carbonate-bound Zn showed a non-significant increase compared to the control ($p > 0.05$), suggesting that biochar–apatite co-amendment does not significantly alter the speciation of zinc towards the carbonate-bound fraction.

This observation aligns with the findings of Vuong *et al.* (2022),[30] who also reported no significant change in the carbonate-bound zinc fraction (F2_Zn) when peanut husk biochar was amended in Pb/Zn-contaminated soils. These results indicate that while biochar–apatite co-amendment may influence the speciation of other metals such as lead, its effect on zinc distribution in the carbonate-bound fraction appears limited. It suggests that the processes responsible for zinc immobilization are not as responsive to pH changes or complexation with carbonate ions in the same way as other metals like lead.

The lack of a significant shift in the F2_Zn fraction suggests that biochar–apatite amendments may not alter zinc speciation in the same way they do for other metals like lead. Zinc forms stable carbonate-bound complexes under high pH, but it can also bind to organic matter or iron/manganese oxides, limiting its shift into the carbonate-bound fraction. In this study, the pH increase from biochar and apatite may not have been sufficient to significantly alter zinc distribution, or biochar may interact differently with zinc compared to lead.

This finding aligns with previous studies showing that biochar's effects on metal speciation depend on factors such as metal type, soil conditions, and biochar properties. While biochar did not significantly affect F2_Zn in this study, it may still immobilize zinc through other mechanisms, such as binding to organic matter or influencing other metal species. Further research is needed to explore these interactions.

3.4.2.3. Fe/Mn-oxide fraction (F3_Zn). The control soil (BS) exhibited an iron/manganese oxide-bound zinc (F3_Zn) concentration of 695.1 ± 41.5 mg kg^{-1}, representing roughly 25% of the total zinc in the soil (Table S4†). Upon biochar–apatite co-amendment, a notable increase in the F3_Zn proportion was observed compared to the control. This suggests that biochar–apatite interactions may play a role in promoting the association of zinc with iron and manganese oxides, potentially enhancing the stabilization of zinc in the soil and reducing its mobility.

This trend aligns with the known ability of biochar to interact with mineral surfaces, particularly iron and manganese oxides, which are well-documented for their high cation-exchange capacity and strong binding affinity for heavy metals. The increased proportion of zinc in the F3_Zn fraction suggests that biochar may facilitate the adsorption of zinc onto these metal oxides, a process that is likely driven by both biochar's surface chemistry and its impact on soil pH. Biochar's inherent surface functional groups, including carboxyl, hydroxyl, and phenolic groups, may interact with the oxides in the soil, promoting the formation of stable zinc-oxide complexes that are less prone to leaching.

Biochar's ability to modify soil pH likely enhances zinc binding to iron and manganese oxides, particularly when combined with apatite. The alkalizing effect promotes the precipitation of these oxides, providing additional binding sites for zinc. This process aligns with previous studies showing that biochar can help immobilize heavy metals like zinc by associating them with iron/manganese oxide fractions.[10,61]

The increase in the F3_Zn fraction suggests that biochar–apatite amendments may reduce zinc mobility by stabilizing it in less bioavailable forms, decreasing the risk of leaching into groundwater or plant uptake. This enhanced stabilization of zinc in the F3 fraction could help mitigate its environmental impact, particularly in areas with zinc contamination.

Overall, biochar–apatite co-amendments appear to effectively influence zinc speciation, promoting its immobilization in more stable forms and offering a potential strategy for managing zinc contamination in soils prone to heavy metal leaching.

3.4.2.4. Organic carbon fraction (F4_Zn). Sequential extraction revealed a relatively low organic matter-bound zinc (F4_Zn) fraction in the control soil (BS), with a concentration of 96.2 ±

2.3 mg kg^{-1}, constituting approximately 2.8% of the total zinc (Fig. 4b). Upon biochar amendment, however, a significant increase in the F4_Zn proportion was observed compared to the control ($p < 0.05$) (Table S4†). The F4_Zn content in co-amended soils ranged from 3.3% to 4.5%, suggesting that biochar plays a more substantial role than apatite in contributing to organic matter-bound zinc in the soil.

These results highlight the ability of biochar to influence the organic carbon fraction of zinc, a mechanism that is often attributed to the interaction between biochar's surface functional groups and the organic matter present in the soil. Biochar, known for its high surface area and reactive functional groups, such as carboxyl, hydroxyl, and phenolic groups, has the potential to adsorb metals, including zinc, onto its surface. This interaction likely enhances the formation of stable zinc-organic matter complexes, which are less bioavailable and less prone to leaching.

In this study, biochar amendment significantly increased the F4_Zn fraction, possibly due to the increased organic matter provided by the biochar itself, along with its surface properties that promote zinc adsorption. The elevated presence of organic carbon in biochar-amended soils may provide additional sites for zinc binding, leading to a higher proportion of zinc being incorporated into the organic matter fraction. This result aligns with previous studies reporting increased F4_Zn upon biochar addition to contaminated soils.[10,62] In these studies, biochar's role in enhancing the F4 fraction was similarly attributed to its capacity to modify the soil's organic carbon content and improve the adsorption of heavy metals like zinc.

In the current study, the increase in F4_Zn observed in the biochar-amended soils suggests that biochar might be particularly effective at promoting the sequestration of zinc in organic carbon fractions, thus reducing its mobility and potential toxicity. While the increase in F4_Zn was modest, it still represents a shift of zinc into a less bioavailable and more stable form, which could help mitigate the environmental risks associated with zinc contamination.

The findings of this study contrast with some prior research that reported minimal or no significant changes in F4_Zn after biochar application.[11,30] These discrepancies could be attributed to differences in biochar characteristics, such as pH, cation-exchange capacity, and the specific organic matter content of the soil used in each study. For example, biochar with a higher pH and electrical conductivity (EC) might exert a more significant impact on zinc adsorption, particularly by increasing the stability of zinc-organic matter complexes. In contrast, biochar with lower pH and EC, as used in this study, may not have as strong an effect on increasing F4_Zn in the short term.

Despite these variations, the increase in organic carbon-bound zinc observed in this study demonstrates that biochar amendments can influence zinc speciation in soils. This finding suggests that biochar could be a viable strategy for mitigating the environmental risks posed by zinc contamination, particularly in situations where stabilizing zinc in less bioavailable forms is a priority.

3.4.2.5. Residual fraction (F5_Zn). The control soil (BS) exhibited a substantial proportion of zinc (Zn) in the residual fraction (F5), with a concentration of 1344.0 ± 23.7 mg kg^{-1}, constituting approximately 39.2% of the total zinc content (Table 3). The residual fraction typically represents the most stable and least bioavailable form of zinc, as it is bound to minerals and other soil components that are not readily mobilized or available for plant uptake. This suggests that the control soil already contained a significant portion of zinc in a less labile, relatively immobile form, potentially posing a lower risk for environmental contamination compared to the more readily available fractions like the exchangeable or carbonate-bound fractions.

However, the introduction of biochar–apatite co-amendment to the soil led to a notable shift in the speciation of zinc, increasing the proportion of zinc in the residual fraction (F5) across the amended soils. Specifically, the proportion of zinc in the F5 fraction ranged from 35.5% to 42.1% in co-amended soils, compared to the 39.2% observed in the control (Fig. 4 and Table S4†). This increase suggests that biochar–apatite co-amendment is effective in promoting the stabilization of zinc in less mobile forms, thereby reducing its bioavailability and potential for leaching.

The most pronounced shift towards the F5 fraction was observed in the TB3_10 sample, where 40.8% of the total zinc was found in the residual fraction. This suggests that the biochar–apatite treatment, particularly at the 10% biochar level, effectively enhanced the stabilization of zinc in the soil. This outcome aligns with previous studies that have reported similar increases in the residual fraction of zinc upon biochar amendment.[10,63] In these studies, biochar's ability to sequester metals in the residual fraction has been attributed to its high surface area, porous structure, and the presence of functional groups that can adsorb and bind metal ions. Additionally, biochar's influence on soil pH and mineral interactions may further promote the immobilization of metals, driving them towards more stable, less bioavailable forms.

The increase in the residual fraction of zinc following biochar–apatite co-amendment highlights the potential of this strategy to reduce zinc mobility and bioavailability while enhancing its sequestration in stable, less bioavailable forms. This shift to the residual fraction lowers the risk of bioaccumulation in plants and aquatic organisms and decreases the potential for zinc leaching into groundwater.

Biochar's adsorptive properties, combined with apatite's ability to form insoluble metal-phosphate complexes, work synergistically to stabilize zinc. This co-amendment approach may provide a long-term solution for managing zinc contamination in soils by locking it in stable forms and reducing its environmental risks.

These findings suggest that biochar–apatite co-amendment is an effective strategy for mitigating zinc contamination, offering both short- and long-term benefits. Further research is needed to assess the long-term stability of zinc in the residual fraction and evaluate the impact on soil health and crop productivity.

3.4.2.6. Summary of key findings. (1) Zn speciation in soil: sequential extraction revealed that Zn speciation in the soil followed a specific order of fractions: F5 (residual fraction) > F3

(Fe/Mn oxide-bound) > F2 (carbonate-bound) > F1 (exchangeable) > F4 (organic carbon-bound). Biochar amendment significantly impacted Zn speciation, with changes observed depending on the application rate.

(2) Exchangeable fraction (F1_Zn): the control soil had a high concentration of exchangeable Zn (F1_Zn), making it mobile and bioavailable. Upon biochar–apatite co-amendment, a significant reduction in this fraction was observed, with the TB3_10 sample showing a 61.5% decrease. This suggests that biochar–apatite interactions effectively reduce Zn mobility, limiting its bioavailability and potential environmental contamination.

(3) Carbonate-bound fraction (F2_Zn): the biochar–apatite amendment did not significantly alter the carbonate-bound Zn fraction, indicating that biochar's effect on Zn speciation is not as pronounced in this fraction. Zinc's behaviour in this fraction may be influenced by other factors, such as its affinity for organic matter or metal oxides.

(4) Fe/Mn-oxide-bound fraction (F3_Zn): biochar–apatite co-amendment increased the proportion of Zn in the Fe/Mn-oxide-bound fraction, suggesting that biochar may facilitate the binding of Zn to iron and manganese oxides. This mechanism helps stabilize Zn, making it less mobile and less bioavailable, thereby reducing its potential for leaching or plant uptake.

(5) Organic carbon-bound fraction (F4_Zn): biochar significantly increased the organic carbon-bound Zn fraction, indicating that biochar promotes the sequestration of Zn in more stable, less bioavailable forms. This effect is attributed to biochar's surface functional groups and its ability to enhance the organic matter content in the soil.

(6) Residual fraction (F5_Zn): biochar–apatite co-amendment increased the proportion of Zn in the residual fraction, particularly at higher biochar concentrations (*e.g.*, TB3_10), suggesting that biochar–apatite treatments enhance the stabilization of Zn in less mobile and less bioavailable forms.

In conclusion, biochar amendment can significantly influence the mobility and bioavailability of soil heavy metals. This impact depends on the specific metal, soil type (including properties like EC, OC, and pH),[9] and biochar properties (feedstock, pyrolysis and composition).[64] The observed impact on exchangeable Pb and Zn likely arises from a confluence of mechanisms, including biochar-induced soil pH increase, ion exchange processes, adsorption, and precipitation (as oxyhydroxides, carbonates, or phosphates).[65]

Prior research consistently demonstrated that biochar application promotes the transformation of mobile, exchangeable heavy metals into more stable forms.[10,11,66] However, the published literature revealed considerable heterogeneity in the observed effects on Pb and Zn speciation following incubation with various biochar types, application rates, and incubation durations.[10,30,61] These variations can likely be attributed to a confluence of factors, including inherent properties of the utilized soil (*e.g.*, texture, mineralogy), the specific biochar characteristics (*e.g.*, feedstock, pyrolysis temperature), and the biochar amendment rate and incubation time.[62]

3.5. Mechanism for immobilizing heavy metals in incubated soil by amendment

The immobilization of heavy metals in the soil through amendments like biochar and apatite involves complex chemical, physical, and biological,[67,68] influenced by the metal type, soil properties, and amendment characteristics. Key mechanisms include adsorption, complexation with biochar's functional groups,[69] cation exchange,[14,70] and precipitation through interactions with phosphate or hydroxide ions,[71,72] This study also examines the role of leaching during a 1–4 weeks incubation period, suggesting that dissolved cations, anions, organic compounds, and small mineral particles from biochar, apatite, and soil may enhance metal immobilization. Additionally, amendments that increase soil pH and electrical conductivity (EC) are found to reduce the exchangeable fraction of metals, with higher biochar amendment rates correlating with greater increases in pH and EC, supporting previous findings[73,74] that alkaline conditions promote metal immobilization.[67,75]

3.5.1. Impact of amendments on soil pH and EC. In this study, all amendments (TSB300, TSB500, and AP) resulted in significantly higher pH values compared to the control soil. This increase in pH promoted hydroxide precipitation reactions, which are well-known to enhance metal immobilization. Specifically, as the soil pH rises, heavy metals such as Pb and Zn may form insoluble hydroxides (*e.g.*, $Pb_3(CO_3)_2(OH)_2$ and $Zn(OH)_2$),[70,76] reducing their bioavailability and mobility within the soil. This provides a clear indication that the elevated pH caused by biochar amendments plays a substantial role in immobilizing heavy metals through precipitation processes. Additionally, biochar's contribution to EC increases the ionic strength in the soil solution, which further promotes the precipitation of these metals into less soluble forms.

3.5.2. Role of biochar's organic functional groups in immobilization. The organic functional groups on the surface of biochar, particularly TSB300, play an essential role in facilitating the immobilization of heavy metals through exchange and complexation reactions. Fourier-Transform Infrared Spectroscopy (FTIR) analysis confirmed the presence of these functional groups, which enhance biochar's ability to adsorb and complex metal ions. The functional groups on TSB300 biochar, including carboxyl, hydroxyl, and phenolic groups, have a high affinity for cationic metals like Pb^{2+} and Zn^{2+}, enabling them to form stable metal–organic complexes. The relatively minor difference observed between TSB300 and TSB500 at identical application rates suggests that both biochar types may rely on their porous surface area and the high pH of TSB300 to mediate metal immobilization, primarily through adsorption and complexation with these functional groups.

3.5.3. Synergistic effects of biochar and apatite co-application. Apatite, a phosphate-rich mineral, has been shown to immobilize Pb^{2+} by facilitating its precipitation with phosphate, forming stable compounds such as $Pb_5(PO_4)_3X$ (where $X = F^-$, Cl^-, Br^-, or OH^-).[77,78] The combination of biochar and apatite creates a synergistic effect, promoting the stabilization of Pb and Zn in soil through a range of mechanisms, including adsorption, ion exchange, complexation, and precipitation.

Apatite's role in binding metals through phosphate formation is particularly crucial in enhancing the long-term stability of the immobilized metals, reducing their potential for leaching into the soil solution.

While apatite does not possess the extensive organic functional groups or high surface area found in biochar, its mineral composition and ability to interact with biochar in a composite amendment significantly enhance its capacity to immobilize heavy metals. The co-application of biochar and apatite results in a combination of organic and inorganic mechanisms that together contribute to the overall immobilization of Pb and Zn, making this composite amendment a promising strategy for heavy metal remediation in contaminated soils.

3.5.4. Formation of stable organic-mineral coatings. A critical aspect of heavy metal immobilization in biochar-amendment-treated soils is the formation of stable organic-mineral coatings on the biochar surface. These coatings develop over the 2–4 weeks incubation period and are believed to be integral to the formation of more stable chemical forms of Pb and Zn in soil. The coatings consist of microaggregates, clusters of mineral nanoparticles and inorganic compounds that are bound together by organic molecules such as humic substances.[10,11,30] These microaggregates facilitate the stabilization of heavy metals within the soil matrix by transforming them into less mobile and less bioavailable forms. This process is especially important in reducing the long-term environmental risks associated with metal-contaminated soils.

3.5.5. EDX and FTIR analysis: evidence of heavy metal immobilization. Energy-dispersive X-ray Spectroscopy (EDX) and Fourier Transform Infrared (FTIR) spectroscopy were employed to further investigate the interaction between heavy metals and biochar during the incubation period. EDX analysis of TSB300 biochar, both before and after 30 days of incubation in soil, provided compelling evidence for the accumulation of Pb and Zn on the biochar surface. As shown in Fig. 5, a distinct increase in the concentrations of Pb and Zn was observed in the post-incubation biochar samples compared to the pre-incubation samples. EDX analysis revealed a distinct elemental signature for the pristine TSB300 biochar, dominated by K, O, C, Ca, Cl, Mg, and P. Conversely, the TSB300 biochar incubated in soil for 30 days exhibited the presence of additional elements, specifically Pb and Zn. This observation is indicative of the accumulation of these heavy metals on the biochar surface, potentially as precipitates or complexes.

To further elucidate the binding mechanisms, FTIR spectra of the biochar samples before and after incubation were analyzed, providing complementary evidence of metal adsorption. The FTIR spectra of TSB300 biochar before and after incubation revealed significant changes, particularly in the carboxyl and hydroxyl functional groups, suggesting interactions between the biochar surface and the metal ions Pb^{2+} and Zn^{2+} (Fig. 6). A noticeable shift in the FTIR peak from 1400 cm^{-1} to 1373 cm^{-1} was observed, which is attributed to the complexation of Pb^{2+} and Zn^{2+} with the carboxyl groups present on the biochar surface. This shift is indicative of surface complexation mechanisms, where the metal ions interact with the oxygen atoms of the carboxyl groups, forming stable bonds. Such interactions are consistent with the findings of previous studies, which have shown that biochar's carboxyl groups play

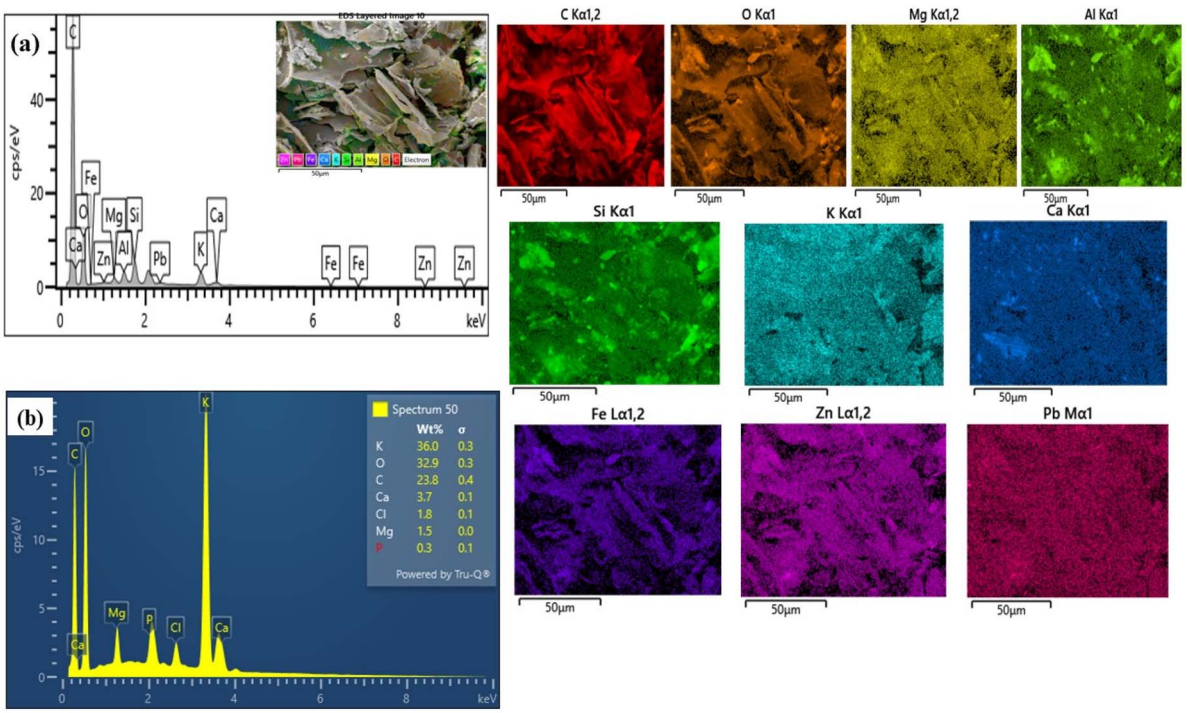

Fig. 5 Energy-dispersive X-ray spectroscopy (EDX) mapping results for elemental distribution in TSB300 biochar samples (a) after 30 days of incubation in the soil at a 10% application rate and (b) before incubation.

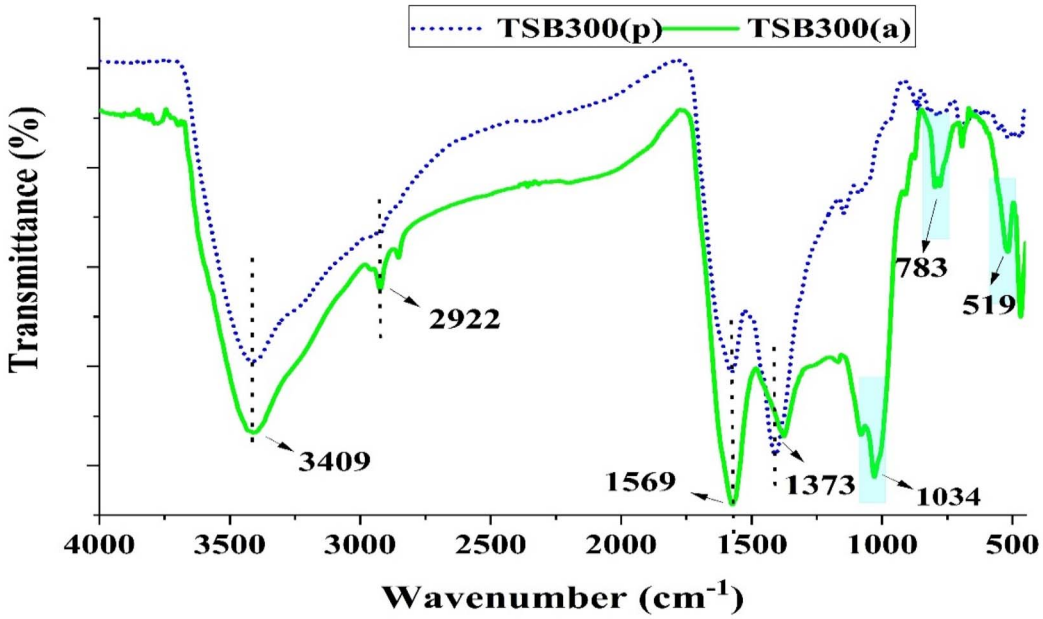

Fig. 6 FT-IR spectra of biochar derived from taro stem at 300 °C before soil incubation (TSB300(p)) and after 30 days of incubation in the soil at a 10% ratio (TSB300(a)).

a significant role in binding metal ions, reducing their mobility and bioavailability in soils.[79]

Furthermore, the appearance of new peaks in the FTIR spectra, specifically in the 768–783 cm^{-1} range, suggests the formation of metal–oxygen complexes. These peaks likely correspond to the bending vibrations of metal–oxygen bonds formed as Pb^{2+} and Zn^{2+} ions adsorb to the biochar surface. The presence of these peaks indicates that biochar's surface functional groups, in conjunction with metal ions, contribute to the formation of stable metal complexes, thereby enhancing the immobilization of these metals.

Additionally, the newly emerged peak at 519 cm^{-1} further supports the idea that Pb^{2+} has been adsorbed onto the biochar surface, forming stable metal–oxygen bonds. This peak likely represents the metal–oxygen stretching vibrations, further confirming the interaction between the biochar surface and Pb^{2+} ions. The emergence of this peak is particularly important, as it suggests that Pb^{2+} ions are strongly bound to the biochar surface, likely in a more stable and less bioavailable form. Similar results have been reported in the literature, where biochar was found to adsorb metal ions, such as Pb^{2+}, through the formation of stable metal–oxygen bonds[10,80]

Together, the EDX and FTIR analyses provide compelling evidence that TSB300 biochar efficiently adsorbs Pb and Zn. The combination of surface adsorption, precipitation, and complexation mechanisms contributes to the immobilization of these heavy metals, reducing their bioavailability and environmental risk. This highlights biochar's potential as a viable soil amendment for remediating Pb and Zn contamination in agricultural or industrial soils.

In conclusion, this study underscores the efficacy of biochar–apatite composites in immobilizing heavy metals through various mechanisms, including precipitation, ion exchange, complexation, and adsorption. The incorporation of biochar enhances soil pH and EC, facilitating metal hydroxide precipitation and the formation of stable metal–organic complexes. The synergistic effects of biochar and apatite further strengthen the immobilization process, transforming Pb and Zn into less mobile and bioavailable forms. Over time, the development of stable organic-mineral coatings on biochar surfaces contributes to the long-term stabilization of these metals. These findings highlight the promise of biochar-based amendments, particularly when combined with apatite, for the effective remediation of heavy metal-contaminated soils.

3.6. Correlation of the exchangeable fraction of lead and zinc with pH, OC, and EC of incubated soil after a one-month incubation

Spearman's correlation analysis was employed to assess the relationships between key soil properties, pH, organic carbon (OC), electrical conductivity (EC), and the exchangeable fractions of lead (Pb) and zinc (Zn) in the incubated soils. The results, presented in Fig. 7a and b, provide significant insights into how these soil properties influence the mobility and availability of Pb and Zn in soils amended with biochar and apatite ore.

3.6.1. Correlation of F1_Pb with soil properties. Fig. 7a illustrates a strong negative correlation between the exchangeable fraction of Pb (F1_Pb) and all three soil properties: pH, OC, and EC, with correlation coefficients (r) of −0.84, −0.80, and −0.85, respectively. These findings suggest that as soil pH, organic carbon content, and electrical conductivity increase, the exchangeable Pb fraction decreases, indicating that higher values of these properties lead to enhanced immobilization of

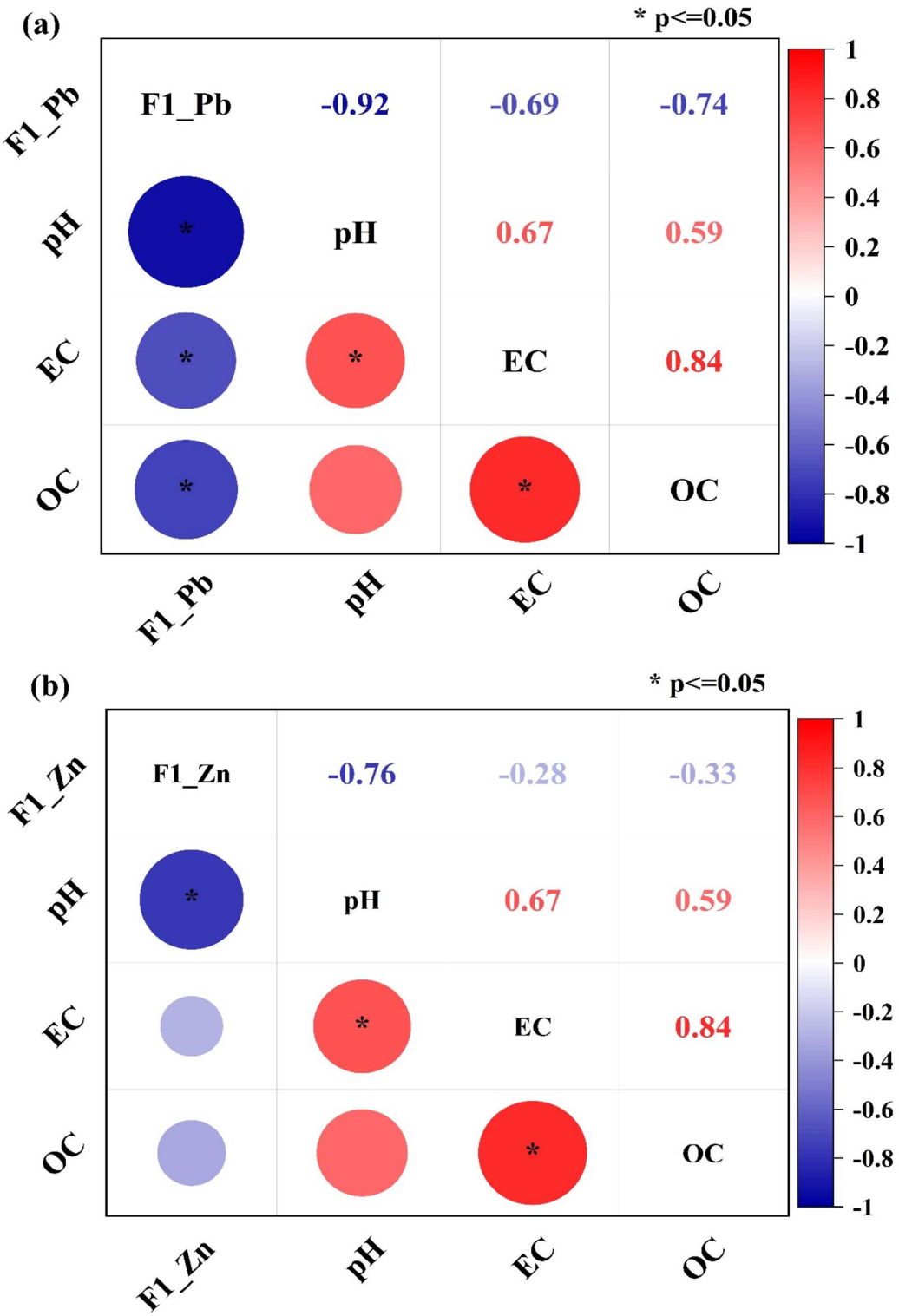

Fig. 7 Correlation analysis of exchangeable Pb (F1_Pb) and Zn (F1_Zn) with soil pH, EC, and OC following one-month biochar and apatite amendment.

Pb and reduced its mobility within the soil solution. This aligns with the general understanding that an increase in pH results in the precipitation of Pb as less soluble forms, such as $Pb(OH)_2$ or Pb-phosphate complexes, which effectively reduce its bioavailability.

The strong negative correlations between F1_Pb and these soil properties suggest that biochar amendment, by raising both soil pH and organic carbon content, may play a crucial role in promoting Pb immobilization. Organic carbon in biochar can act as a sorbent for Pb ions, potentially through surface

interactions or cation exchange mechanisms, thus reducing the exchangeable Pb fraction.

3.6.2. Correlation of F1_Zn with soil properties. Fig. 7b presents the correlation between the exchangeable fraction of Zn (F1_Zn) and soil properties. A strong negative correlation was observed between F1_Zn and pH ($r = -0.76$), indicating that as soil pH increases, exchangeable Zn decreases. This relationship suggests that higher soil pH promotes the precipitation of Zn as insoluble compounds, such as zinc hydroxides or phosphates, thereby reducing its mobility in the soil solution. This is in line with the general trend observed for Pb, indicating that the mechanisms of metal immobilization in response to changes in soil pH might be similar for both Pb and Zn.

However, the correlations between F1_Zn and both EC ($r = -0.28$) and OC ($r = -0.33$) were relatively weak and negative, which suggests that while soil organic carbon and electrical conductivity may influence Zn availability, the effect is less pronounced than for Pb. This could be attributed to the different geochemical behaviors of Zn compared to Pb, as Zn tends to be more mobile and soluble under a wider range of soil conditions. Moreover, the lower negative correlation between F1_Zn and EC might reflect the fact that Zn's mobility in soil is influenced not only by EC but also by other factors such as its interaction with soil mineral phases and organic matter.

3.6.3. Correlations between soil properties (pH, OC, and EC). A noteworthy finding in Fig. 7a is the significant positive correlation observed between soil pH and both OC ($r = +0.67$) and EC ($r = +0.59$). This suggests that higher organic carbon content, often introduced by biochar, is associated with increased pH and EC. The increase in pH could be a result of the alkaline nature of biochar, which has been shown to elevate soil pH upon application, potentially through the release of basic cations like calcium (Ca^{2+}) and magnesium (Mg^{2+}) from biochar's structure. Additionally, the increase in EC may be linked to the release of soluble ions from biochar, enhancing the ionic strength of the soil solution, which in turn could affect metal solubility and mobility.

The strong positive correlation between EC and OC ($r = +0.84$) supports the hypothesis that biochar, as a source of organic carbon, contributes to both the increase in soil organic matter and the rise in electrical conductivity. This finding is critical because the interaction between organic matter and soil electrolytes may play an essential role in modulating the availability and mobility of metals like Pb, potentially improving the effectiveness of biochar in soil remediation.

3.6.4. Comparison with previous studies. The observed correlations between the exchangeable fractions of both Pb and Zn with soil pH, OC, and EC are consistent with previous studies that examined biochar-treated Pb- and Zn-contaminated soils. Prior research has demonstrated negative correlations between F1_Pb and F1_Zn with soil pH, OC, and EC, highlighting the potential of biochar as an amendment for enhancing heavy metal immobilization in contaminated soils.[10,11,18,29] The negative correlations with pH in particular support the hypothesis that biochar's ability to raise soil pH is a key mechanism through which it promotes metal immobilization.

However, the distinct correlation patterns for Pb and Zn may reflect the different chemical forms and bioavailability of these metals in the soil. For example, while both metals form insoluble precipitates at higher pH, Pb tends to form more stable, less mobile complexes, whereas Zn is more readily soluble in neutral to slightly alkaline conditions. This may explain the stronger correlations between Pb and pH, OC, and EC, compared to Zn.

In conclusion, the correlation analysis reveals that soil pH plays a critical role in the immobilization of both Pb and Zn, with biochar and apatite amendments enhancing metal sequestration through increases in pH, organic carbon content, and electrical conductivity. Strong negative correlations between exchangeable Pb and soil properties, especially pH, suggest that biochar effectively reduces Pb mobility by promoting precipitation and complexation. In contrast, while soil pH significantly affects Zn, the weaker correlations with organic carbon and electrical conductivity indicate that other factors, such as the specific geochemical behaviour of Zn, may influence its availability in soil. These findings highlight the potential of biochar amendments, particularly in combination with apatite, for the long-term immobilization of heavy metals in contaminated soils, with implications for improving soil remediation strategies. Further research is needed to explore Zn-specific mechanisms and optimize biochar applications for broader metal contaminants.

3.7. Principal component analysis (PCA) and its interpretation

Principal Component Analysis (PCA) was employed to assess the relationships between the exchangeable fractions of lead (F1_Pb) and zinc (F1_Zn) and key soil properties, including pH, organic carbon (OC), and electrical conductivity (EC), following the amendment period. The outcomes of the PCA, summarized in Table 6 and Fig. 8, provide valuable insights into the interrelationships between the variables and the dynamics of metal mobility in amended soils. PCA is particularly useful in reducing the dimensionality of the dataset while retaining the most important information, thus offering a clearer understanding of how multiple variables interact with each other.

The component loadings, represented as correlation coefficients, indicate how each original variable contributes to the formation of a principal component (PC). A positive loading

Table 6 Component matrix showing the influence of organic carbon (OC), pH, and electrical conductivity (EC) on exchangeable fraction of lead (F1_Pb) and zinc (F1_Zn)

Element	Component 1	Component 2
F1_Pb	−0.48746	−0.03494
F1_Zn	−0.34651	0.76614
pH	0.46407	−0.27503
EC	0.47012	0.36561
OC	0.45379	0.44998
Eigenvalue	3.92664	0.84122
Cumulative variances (%)	78.53%	95.36%

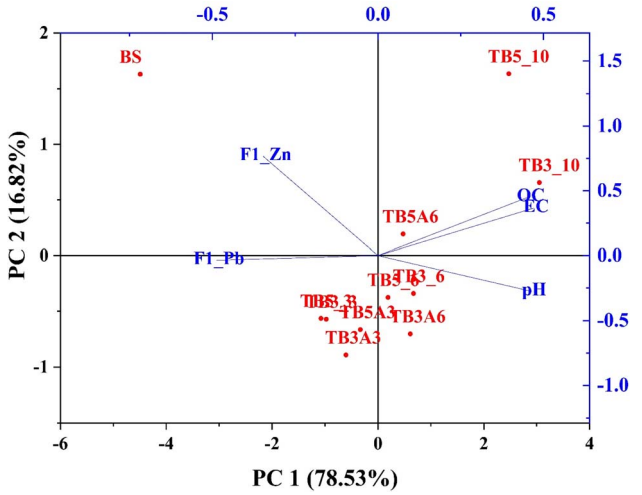

Fig. 8 PCA results show the relationships between pH, EC, and OC with the exchangeable fractions of Pb and Zn of incubated soil samples in a two-dimensional loading plot.

suggests that as the value of the variable increases, the value of the corresponding principal component also increases, while a negative loading suggests an inverse relationship. By examining these loadings, we can gain a comprehensive understanding of how the exchangeable fractions of Pb and Zn relate to key soil properties such as pH, OC, and EC.

3.7.1. Interpretation of the first principal component (PC1). The first principal component (PC1) accounts for 78.53% of the total variance in the dataset, which is a significant proportion and indicates that it captures the majority of the variability in the data. The negative loadings for both F1_Pb (−0.48746) and F1_Zn (−0.34651) suggest a strong inverse relationship between the exchangeable fractions of Pb and Zn and key soil properties like pH, OC, and EC. This negative correlation implies that as soil pH, organic carbon content, and electrical conductivity increase, the mobility and bioavailability of Pb and Zn decrease. The reduction in the exchangeable fractions of these metals signifies enhanced immobilization, suggesting that these soil properties play a vital role in the transformation of Pb and Zn from more mobile forms to less bioavailable forms, such as precipitates or sorbed complexes, which are less likely to leach into groundwater or be taken up by plants.

The strong negative loadings for both F1_Pb and F1_Zn on PC1 support the idea that biochar–apatite co-amendment may be effective in reducing the environmental risks associated with Pb and Zn contamination by improving soil properties. By increasing soil pH (due to the alkaline nature of biochar), organic carbon (*via* biochar's contribution), and EC (through the ionic release from biochar), the mobility of these heavy metals can be significantly reduced. This reduction in metal bioavailability not only reduces toxicity to plants and soil organisms but also improves overall soil health by mitigating the adverse effects of metal toxicity.

3.7.2. Correlations between soil properties on PC1. The positive loadings for soil properties such as pH (+0.46407), organic carbon (OC) (+0.45379), and electrical conductivity (EC) (+0.47012) on PC1 further corroborate the inverse relationship with the exchangeable fractions of Pb and Zn. These positive loadings indicate that as these soil properties increase, the corresponding PC1 value also increases, leading to lower exchangeable Pb and Zn levels.

3.7.2.1. Soil pH. The positive loading of pH indicates that higher pH levels are associated with the decreased mobility of Pb and Zn. This is consistent with the known fact that at higher pH levels, Pb and Zn are more likely to form insoluble hydroxides or phosphate complexes, which are less mobile and bioavailable. Therefore, raising soil pH through biochar application can help sequester these metals in less available forms, thereby reducing their toxic effects.

3.7.2.2. Organic carbon (OC). The positive loading of OC suggests that organic carbon, particularly from biochar, enhances the binding and immobilization of Pb and Zn. Biochar's surface chemistry, including its high cation-exchange capacity and presence of functional groups, allows it to adsorb heavy metals, thereby reducing their exchangeable fractions in the soil. Moreover, OC can also support microbial activity that promotes the transformation of metals into less mobile forms.

3.7.2.3. Electrical conductivity (EC). The positive correlation between EC and reduced F1_Pb and F1_Zn levels suggests that increased ionic strength in the soil (due to biochar's influence on EC) helps in metal precipitation. The release of soluble ions from biochar may facilitate the formation of insoluble metal salts, further decreasing the metals' bioavailability.

3.7.3. Interpretation of the second principal component (PC2). PC2 accounts for 16.83% of the total variance in the dataset, which is a smaller proportion compared to PC1 but still offers useful information regarding the relationships between soil properties. The positive loading for pH (+0.46407) on PC2 suggests that this component is associated with higher pH levels in the soil, reinforcing the importance of pH in influencing metal availability. Conversely, the negative loading for OC (−0.44998) on PC2 suggests that, in this component, higher pH levels tend to be associated with lower OC content. This inverse relationship could arise from soil processes such as mineralization or microbial decomposition, where higher pH environments may promote the breakdown of organic material and thus reduce OC levels.

This finding suggests that there may be a trade-off between pH and OC content in some soils, which could be important when managing soil conditions for optimal heavy metal immobilization. For example, while raising soil pH can be beneficial for reducing Pb and Zn bioavailability, it may also decrease organic carbon levels, which could reduce the soil's ability to immobilize metals *via* organic matter. Therefore, it is crucial to strike a balance between pH and organic carbon content to maximize the effectiveness of biochar in immobilizing heavy metals while maintaining soil health.

3.7.4. Summary of principal component analysis results. Inclusion, the PCA results highlight the significant role that soil properties, particularly pH, OC, and EC, play in the immobilization of Pb and Zn. The strong inverse correlation between the

exchangeable fractions of these metals and the soil properties suggests that improving soil quality—characterized by higher pH, organic carbon content, and electrical conductivity—leads to a reduction in metal mobility, thus enhancing their immobilization in contaminated soils.

Furthermore, the analysis of PC2 emphasizes the complex interactions between pH and OC, suggesting that soil management strategies should carefully consider both properties to optimize metal immobilization. Biochar–apatite co-amendments offer a promising solution by improving these key soil properties, which may help reduce the bioavailability and toxicity of Pb and Zn in contaminated soils. Future research should explore the balance between pH and organic carbon content in more detail, as well as investigate the interactions between different types of soil amendments and their long-term effects on metal immobilization.

4. Conclusions

4.1. Characterization of biochar and apatite

The biochar samples (TSB300 and TSB500) and apatite were analyzed for their potential in soil remediation. Both amendments displayed elevated pH levels and low concentrations of Pb and Zn, indicating their suitability for mitigating heavy metal contamination. Further characterization through FTIR, SEM-EDS, and BET analyses revealed that TSB300 contained a higher abundance of functional groups and a greater surface area compared to TSB500. This increased surface area in TSB300 likely enhances its capacity for metal adsorption, making it a potentially more effective amendment for soil remediation.

4.2. Effect on soil properties

After a 30-day incubation period, biochar and apatite amendments led to significant improvements in soil properties, as indicated by increased pH, organic carbon (OC), and electrical conductivity (EC) when compared to untreated controls. These changes suggest that the amendments have a positive impact on soil health, potentially enhancing both the fertility and environmental conditions of contaminated soils.

4.3. Impact on Pb and Zn chemical fractions

The incubation of soil with varying application rates of TSB300, TSB500, and apatite resulted in notable changes in the chemical fractions of Pb and Zn. There was a significant reduction in the exchangeable fractions (F1) of both metals, with Pb decreasing by up to 71.8% and Zn by up to 61.5%. In contrast, there were corresponding increases in the more stable fractions (F4 and F5). These results highlight the potential for biochar and apatite amendments to reduce the bioavailability of heavy metals in soil by shifting them to more stable, less mobile forms.

4.4. Mechanisms of heavy metal immobilization

The reduction in the exchangeable fractions of Pb and Zn likely results from a combination of processes, including cation exchange, precipitation, and adsorption on the biochar surface. Both biochar types demonstrated similar effects, suggesting that comparable mechanisms may be at play, although further studies are needed to fully elucidate the relative contributions of each process.

4.5. Future research directions

Future research should focus on examining the long-term stability of heavy metal immobilization in biochar-amended soils and assessing the effects of these amendments on soil microbial communities and overall ecosystem functions. Long-term field trials would also be valuable to assess the durability of these amendments beyond the laboratory conditions.

Data availability

All data obtained have been included in the manuscript, in the ESI,† and are available from the corresponding author upon reasonable request.

Author contributions

Conceptualization: T. X. V.; methodology: D. P. N. and N. V. H. N.; software: T. T. H. P. and T. T. T. N.; validation: T. X. V. and D. P. N.; data curation: T. X. V. , D. P. N. and N. V. H. N.; writing original draft preparation, T. X. V. and T. T. H. P. and T. T. T. N.; writing – review and editing, V. T. X.: visualization: N. Đ. P. and V. H. N. All authors have read and agreed to the published version of the manuscript.

Conflicts of interest

The authors declare no conflicts of interest.

References

1 K. H. Hama Aziz, *et al.*, Heavy metal pollution in the aquatic environment: efficient and low-cost removal approaches to eliminate their toxicity: a review, *RSC Adv.*, 2023, **13**, 17595–17610.
2 C. Zamora-Ledezma, *et al.*, Heavy metal water pollution: a fresh look about hazards, novel and conventional remediation methods, *Environ. Technol. Innov.*, 2021, **22**, 101504.
3 H. Gui, *et al.*, Spatial distribution, contamination characteristics and ecological-health risk assessment of toxic heavy metals in soils near a smelting area, *Environ. Res.*, 2023, **222**, 115328.
4 M. S. Chaithanya, B. Das and R. Vidya, Distribution, chemical speciation and human health risk assessment of metals in soil particle size fractions from an industrial area, *J. Hazard. Mater. Adv.*, 2023, **9**, 100237.
5 Y. Lu, W. Yin, L. Huang, G. Zhang and Y. Zhao, Assessment of bioaccessibility and exposure risk of arsenic and lead in urban soils of Guangzhou City, China, *Environ. Geochem. Health*, 2011, **33**, 93–102.

6 M. Narayanan and Y. Ma, Influences of Biochar on Bioremediation/Phytoremediation Potential of Metal-Contaminated Soils, *Front. Microbiol.*, 2022, **13**, 929730.
7 W. Wang, X. Wang, H. Zhang, Q. Shi and H. Liu, Rhamnolipid-Enhanced ZVI-Activated Sodium Persulfate Remediation of Pyrene-Contaminated Soil, *Int. J. Environ. Res. Public Health*, 2022, **19**, 11518.
8 C. S. Lwin, B. H. Seo, H. U. Kim, G. Owens and K. R. Kim, Application of soil amendments to contaminated soils for heavy metal immobilization and improved soil quality—a critical review, *Soil Sci. Plant Nutr.*, 2018, **64**, 156–167.
9 M. Awad, *et al.*, Diminishing heavy metal hazards of contaminated soil *via* biochar supplementation, *Sustain*, 2021, **13**, 1–14.
10 T. T. T. Nguyen, *et al.*, Lead and zinc chemical fraction alterations in multi-metal contaminated soil with pomelo peel biochar and biochar/apatite incubation, *Mater. Res. Express*, 2024, **11**, 045602.
11 V. M. Dang, *et al.*, Immobilization of heavy metals in contaminated soil after mining activity by using biochar and other industrial by-products: the significant role of minerals on the biochar surfaces, *Environ. Technol.*, 2019, **40**, 3200–3215.
12 A. Tessier, P. G. C. Campbell and M. Bisson, Sequential Extraction Procedure for the Speciation of Particulate Trace Metals, *Anal. Chem.*, 1979, **51**, 844–851.
13 W. Cui, X. Li, W. Duan, M. Xie and X. Dong, Heavy metal stabilization remediation in polluted soils with stabilizing materials: a review, *Environ. Geochem. Health*, 2023, **45**, 4127–4163.
14 Y. Wang, H. S. Wang, C. S. Tang, K. Gu and B. Shi, Remediation of heavy-metal-contaminated soils by biochar: a review, *Environ. Geotech.*, 2019, **9**, 135–148.
15 S. Cheng, *et al.*, Application Research of Biochar for the Remediation of Soil Heavy Metals Contamination: A Review, *Molecules*, 2020, **25**, 1–21.
16 K. Barčauskaitė, *et al.*, Determination of Heavy Metals Immobilization by Chemical Fractions in Contaminated Soil Amended with Biochar, *Sustain*, 2023, **15**, 8677.
17 M. S. Rashid, *et al.*, Assessing the influence of sewage sludge and derived-biochar in immobilization and transformation of heavy metals in polluted soil: impact on intracellular free radical formation in maize, *Environ. Pollut.*, 2022, **309**, 119768.
18 X. T. Vuong, *et al.*, Impacts of sugarcane bagasse - derived biochar and apatite on heavy metal speciation in incubated heavy metal - contaminated soil, *Environ. Sci. Pollut. Res.*, 2025, 1–28.
19 L. Liu, W. Li, W. Song and M. Guo, Remediation techniques for heavy metal-contaminated soils: principles and applicability, *Sci. Total Environ.*, 2018, **633**, 206–219.
20 H. Li, *et al.*, Mechanisms for potential Pb immobilization by hydroxyapatite in a soil-rice system, *Sci. Total Environ.*, 2021, **783**, 147037.
21 Z. Li, *et al.*, Application of apatite particles for remediation of contaminated soil and groundwater: a review and perspectives, *Sci. Total Environ.*, 2023, **904**, 166918.
22 X. Chen, J. V. Wright, J. L. Conca and L. M. Peurrung, Evaluation of heavy metal remediation using mineral apatite, *Water. Air. Soil Pollut.*, 1997, **98**, 57–78.
23 Z. Yang, *et al.*, Iron-doped hydroxyapatite for the simultaneous remediation of lead-, cadmium- and arsenic-co-contaminated soil, *Environ. Pollut.*, 2022, **312**, 119953.
24 X. Chen, J. V. Wright, J. L. Conca and L. M. Peurrung, Effects of pH on heavy metal sorption on mineral apatite, *Environ. Sci. Technol.*, 1997, **31**, 624–631.
25 S. Joseph, *et al.*, How biochar works, and when it doesn't: a review of mechanisms controlling soil and plant responses to biochar, *GCB Bioenergy*, 2021, **13**, 1731–1764.
26 C. Peiris, *et al.*, Phosphorus-enriched biochar for the remediation of heavy metal contaminated soil, *J. Agric. Food Res.*, 2023, **12**, 100546.
27 X. T. Vuong, *et al.*, Speciation and environmental risk assessment of heavy metals in soil from a lead/zinc mining site in Vietnam, *Int. J. Environ. Sci. Technol.*, 2023, **20**, 5295–5310.
28 V. M. Dang, *et al.*, Evaluation of fly ash, apatite and rice straw derived-biochar in varying combinations for *in situ* remediation of soils contaminated with multiple heavy metals, *Soil Sci. Plant Nutr.*, 2020, **66**, 379–388.
29 T. X. Vuong, J. Stephen, T. T. T. Nguyen, V. Cao and D. T. N. Pham, Insight into the Speciation of Heavy Metals in the Contaminated Soil Incubated with Corn Cob-Derived Biochar and Apatite, *Molecules*, 2023, **28**, 2225.
30 T. X. Vuong, *et al.*, Chemical Fractionations of Lead and Zinc in the Contaminated Soil Amended with the Blended Biochar/Apatite, *Molecules*, 2022, **27**, 8044.
31 H. Zhou, *et al.*, Effect of biochar and humic acid on the copper, lead, and cadmium passivation during composting, *Bioresour. Technol.*, 2018, **258**, 279–286.
32 W. P. Miller and D. M. Miller, A micro-pipette method for soil mechanical analysis, *Commun. Soil Sci. Plant Anal.*, 1987, **18**, 1–15.
33 A. Walkley and I. A. Black, An examination of the degtjareff method for determining soil organic matter, and a proposed modification of the chromic acid titration method, *Soil Sci.*, 1934, **37**, 29–38.
34 QCVN03-MT:2005/BTNMT), *QCVN 03-MT: 2015/BTNMT Quy Chuẩn kỹ thuật quốc gia*, 2015.
35 M. B. McBride, *Environna Ental Chemistry of So|| LS*, Environna Ental Chem. So|| LS, 1994.
36 A. Kali, *et al.*, Characterization and adsorption capacity of four low-cost adsorbents based on coconut, almond, walnut, and peanut shells for copper removal, *Biomass Convers. Biorefin.*, 2022, **14**, 3655–3666.
37 W. Tao, *et al.*, An integrated study on the pyrolysis mecanism of peanut shell based on the kinetic analysis and solid/gas characterization, *Bioresour. Technol.*, 2021, **329**, 124860.
38 A. Y. Elnour, *et al.*, Effect of pyrolysis temperature on biochar microstructural evolution, physicochemical characteristics, and its influence on biochar/polypropylene composites, *Appl. Sci.*, 2019, **9**, 7–9.
39 E. Behazin, *et al.*, Mechanical, chemical, and physical properties of wood and perennial grass biochars for

possible composite application, *Bioresour.*, 2016, **11**, 1334–1348.
40 G. Liu, *et al.*, Partitioning and geochemical fractions of heavy metals from geogenic and anthropogenic sources in various soil particle size fractions, *Geoderma*, 2018, **312**, 104–113.
41 G. Liu, H. Zheng, Z. Jiang and Z. Wang, Effects of biochar input on the properties of soil nanoparticles and dispersion/sedimentation of natural mineral nanoparticles in aqueous phase, *Sci. Total Environ.*, 2018, **634**, 595–605.
42 H. Huang, *et al.*, Effect of pyrolysis temperature on chemical form, behavior and environmental risk of Zn, Pb and Cd in biochar produced from phytoremediation residue, *Bioresour. Technol.*, 2017, **249**, 487–493.
43 P. T. Nguyen, *et al.*, Treatment of Cd^{2+} and Cu^{2+} Ions Using Modified Apatite Ore, *J. Chem.*, 2020, **1**, 6527197.
44 I. Nikčević, *et al.*, Mechanochemical synthesis of nanostructured fluorapatite/fluorhydroxyapatite and carbonated fluorapatite/fluorhydroxyapatite, *J. Solid State Chem.*, 2004, **177**, 2565–2574.
45 A. P. L. Nunes, A. E. C. Peres, A. P. Chaves and W. R. Ferreira, Effect of alkyl chain length of amines on fluorapatite and aluminium phosphates floatabilities, *J. Mater. Res. Technol.*, 2019, **8**, 3623–3634.
46 M. Wang, R. Qian, M. Bao, C. Gu and P. R. Zhu, FT-IR and XRD study of bovine bone mineral and carbonated apatites with different carbonate levels, *Mater. Lett.*, 2018, **210**, 203–206.
47 M. Uchimiya, L. H. Wartelle, K. T. Klasson, C. A. Fortier and I. M. Lima, Influence of pyrolysis temperature on biochar property and function as a heavy metal sorbent in soil, *J. Agric. Food Chem.*, 2011, **59**, 2501–2510.
48 M. Zhao, *et al.*, Mechanisms of Pb and/or Zn adsorption by different biochars: Biochar characteristics, stability, and binding energies, *Sci. Total Environ.*, 2020, **717**, 136894.
49 J. Bayar, *et al.*, Biochar-based adsorption for heavy metal removal in water: a sustainable and cost-effective approach, *Environ. Geochem. Health*, 2024, **46**, 428.
50 M. Nazeer, M. J. Khan, D. Muhammad and A. Khan, Biochar application stabilized the heavy metals in coal mined soil, *Can. J. Soil Sci.*, 2022, **103**, 297–304.
51 X. Zhao, *et al.*, Application of Biochar in the Remediation of Contaminated Soil with High Concentration of Lead and Zinc, *Adv. Civ. Eng.*, 2021, **2021**, 6630982.
52 A. P. Puga, L. C. A. Melo, C. A. de Abreu, A. R. Coscione and J. Paz-Ferreiro, Leaching and fractionation of heavy metals in mining soils amended with biochar, *Soil Tillage Res.*, 2016, **164**, 25–33.
53 R. H. Zhang, *et al.*, Immobilization and bioavailability of heavy metals in greenhouse soils amended with rice straw-derived biochar, *Ecol. Eng.*, 2017, **98**, 183–188.
54 M. Uchimiya, S. C. Chang and K. T. Klasson, Screening biochars for heavy metal retention in soil: Role of oxygen functional groups, *J. Hazard. Mater.*, 2011, **190**, 432–441.
55 V. M. Dang, *et al.*, Evaluation of fly ash, apatite and rice straw derived-biochar in varying combinations for *in situ* remediation of soils contaminated with multiple heavy metals, *Soil Sci. Plant Nutr.*, 2020, **66**, 379–388.
56 A. Vannini, *et al.*, Biochar amendment reduces the availability of Pb in the soil and its uptake in lettuce, *Toxics*, 2021, **9**, 268.
57 E. N. Bulanov, A. A. Vasileva, O. N. Golitsyna, A. G. Shvareva and A. V. Knyazev, Search for new apatite-like phases for lead utilization based on crystal structure and thermal expansion, *J. Serb. Chem. Soc.*, 2024, **89**, 415–428.
58 O. Hassanzadeh Moghimi, G. Nabi Bidhendi, A. Daryabeigi Zand, M. Rabiee Abyaneh and A. Nabi Bidhendi, Effect of forest-based biochar on maturity indices and bio-availability of heavy metals during the composting process of organic fraction of municipal solid waste (OFMSW), *Sci. Rep.*, 2023, **13**, 15977.
59 I. Ibrahim, T. Tsubota, M. A. Hassan and Y. Andou, Surface functionalization of biochar from oil palm empty fruit bunch through hydrothermal process, *Processes*, 2021, **9**, 1–14.
60 J. Liang, *et al.*, Changes in heavy metal mobility and availability from contaminated wetland soil remediated with combined biochar-compost, *Chemosphere*, 2017, **181**, 281–288.
61 T. X. Vuong, T. T. H. Pham, T. T. T. Nguyen and D. T. N. Pham, Effects of Biochar and Apatite on Chemical Forms of Lead and Zinc in Multi-Metal-Contaminated Soil after Incubation: A Comparison of Peanut Shell and Corn Cob Biochar, *Sustain*, 2023, **15**, 11992.
62 X. Chao, *et al.*, Effect of biochar from peanut shell on speciation and availability of lead and zinc in an acidic paddy soil, *Ecotoxicol. Environ. Saf.*, 2018, **164**, 554–561.
63 M. Ahmad, *et al.*, Phosphorus-loaded biochar changes soil heavy metals availability and uptake potential of maize (*Zea mays L.*) plants, *Chemosphere*, 2018, **194**, 327–339.
64 A. Karimi, A. Moezzi, M. Chorom and N. Enayatizamir, Chemical Fractions and Availability of Zn in a Calcareous Soil in Response to Biochar Amendments, *J. Soil Sci. Plant Nutr.*, 2019, **19**, 851–864.
65 S. Dai, *et al.*, Effects of biochar amendments on speciation and bioavailability of heavy metals in coal-mine-contaminated soil, *Hum. Ecol. Risk Assess.*, 2018, 1–14.
66 T. X. Vuong, J. Stephen, T. T. T. Nguyen, V. Cao and D. T. N. Pham, Insight into the Speciation of Heavy Metals in the Contaminated Soil Incubated with Corn Cob-Derived Biochar and Apatite, *Molecules*, 2023, **28**, 2225.
67 S. Lei, Y. Shi, Y. Qiu, L. Che and C. Xue, Performance and mechanisms of emerging animal-derived biochars for immobilization of heavy metals, *Sci. Total Environ.*, 2019, **646**, 1281–1289.
68 H. Lu, *et al.*, Relative distribution of Pb^{2+} sorption mechanisms by sludge-derived biochar, *Water Res.*, 2012, **46**, 854–862.
69 M. Huang, *et al.*, Compost as a Soil Amendment to Remediate Heavy Metal-Contaminated Agricultural Soil: Mechanisms, Efficacy, Problems, and Strategies, *Water, Air, Soil Pollut.*, 2016, **227**, 1–18.
70 S. Cheng, *et al.*, Application research of biochar for the remediation of soil heavy metals contamination: a review, *Molecules*, 2020, **25**, 3167.

71 J. H. Park, *et al.*, Comparative Sorption of Pb and Cd by Biochars and Its Implication for Metal Immobilization in Soils, *Water. Air. Soil Pollut.*, 2013, **224**, 1–13.
72 K. B. Cantrell, P. G. Hunt, M. Uchimiya, J. M. Novak and K. S. Ro, Impact of pyrolysis temperature and manure source on physicochemical characteristics of biochar, *Bioresour. Technol.*, 2012, **107**, 419–428.
73 K. Lu, *et al.*, Effect of bamboo and rice straw biochars on the mobility and redistribution of heavy metals (Cd, Cu, Pb and Zn) in contaminated soil, *J. Environ. Manage.*, 2017, **186**, 285–292.
74 M. Awad, *et al.*, Fractionation of heavy metals in multi-contaminated soil treated with biochar using the sequential extraction procedure, *Biomolecules*, 2021, **11**, 1–13.
75 K. M. Banat, F. M. Howari and M. M. To'mah, Chemical fractionation and heavy metal distribution in agricultural soils, north of Jordan Valley, *Soil Sediment Contam.*, 2007, **16**, 89–107.
76 H. Lin, G. Li, Y. Dong and J. Li, Effect of pH on the release of heavy metals from stone coal waste rocks, *Int. J. Miner. Process.*, 2017, **165**, 1–7.
77 S. Mehmood, *et al.*, Impact of different amendments on biochemical responses of sesame (*Sesamum indicum L.*) plants grown in lead-cadmium contaminated soil, *Plant Physiol. Biochem.*, 2018, **132**, 345–355.
78 S. Mehmood, *et al.*, Leaching Behavior of Pb and Cd and Transformation of Their Speciation in Co-Contaminated Soil Receiving Different Passivators, *Environ. Eng. Sci.*, 2019, **36**, 749–759.
79 Y. Deng, *et al.*, Synthesis of magnesium modified biochar for removing copper, lead and cadmium in single and binary systems from aqueous solutions: Adsorption mechanism, *Water*, 2021, **13**, 1–15.
80 Q. Wu, *et al.*, Adsorption characteristics of Pb(II) using biochar derived from spent mushroom substrate, *Sci. Rep.*, 2019, **9**, 15999.